UNIVERSITY OF
KWAZULU-NATAL

INYUVESI
YAKWAZULU-NATALI

Characterizing the Function of the *Rv3218* Gene in *Mycobacterium tuberculosis*

Khumbuzile Canham

220061969

Submitted in fulfilment of the requirements for the degree of

Masters in Medical Science (Medical Microbiology)

Discipline of Medical Microbiology

School of Laboratory Medicine and Medical Sciences

College of Health Sciences

University of KwaZulu-Natal

2023

Student: **Date: 30/03/2023**

Supervisor: **Date: 30/03/2023**

DECLARATION

This study represents original work by the Author, and has not been submitted in any other form to another University. Where use of other work by others was used, it has been duly acknowledged in the text.

_____

Signed by: Khumbuzile Canham

Date: 30/03/2023

DEDICATION

To my beloved Family, ooSukude!!!

ACKNOWLEDGEMENTS

"When the time is right, I, the Lord, will make it happen", Isaiah 60:22.

First and foremost, I would like to express my gratitude to my Lord and Almighty Saviour for being my fortress and for giving me patience and wisdom to complete this master's degree.

I would like to sincerely give my warmest thank to my Supervisor, Dr Sibusiso Senzani for his Scientific contributions, guidance, and an opportunity to conduct this research under his supervision. It was a great honour and privilege working under your professional supervision.

I would also like to thank the Department of Medical Microbiology at large for welcoming me and for giving me emotional support when I needed it. I would like to thank them for assisting with my training and allowing me an opportunity to conduct my experiments on their laboratories.

My sincerest gratitude also goes to my colleagues and friends; thank you so much for sharing your scientific knowledge with me and assisting me where you could.

I would like to acknowledge the project funding provided by the National Research Foundation (Grantholder-linked and DST-NRF Innovation Masters Bursary) and the UKZN College of Health Sciences.

Table of Contents

LIST OF TABLES

LIST OF FIGURES

LIST OF ABBREVIATIONS

Abbreviation	**Full name**
ADP	Adenosine di-phosphate
AGP	Arabinogalactan phosphate
ATc	AnhydroTetracycline
ATP	Adenosine Tri Phosphate
BCG	Bacillus Calmette-Guérin
BLAST	Basic Local Allignment Search Tool
BREC	Biomedical Research Ethics Committee
BDQ	Bedaquiline
^{o}C	Degrees Celsius
$CaCl_2$	Calcium Chloride
CDC	Centre for Disease Control
CFu	Colony forming units

CRISPRI	Clustered Regularly Interspaced Short Palindromic Sequence
CTAB	Cetyltrimethylammonium bromide
DAG	Diacylglycerol
Dec-P	Decaprenyl phosphate
DGK	Diacylglycerol Kinase
DNA	Deoxyribonucleic acid
DTT	Dithiothreitol
ECM	Extracellular matrix
E. coli	*Escherichia Coli*
EMB	Ethambutol
ETZ	Electron Transparent Zone
g	G-Force/ Relative Centrifugal Force
HP	Hypothetical Protein
Hrs	Hours
IM	Inner/plasma membrane
IMP	Ionsine monophosphate
INH	Isoniazid
kDa	Kilo Dalton
KZN	KwaZulu-Natal
Mbp	Million base pairs
MDO	Membrane-Derived Oligonuceotide
MDR	Multidrug-resistant
MFX	Moxifloxacin
$Mg2^{+}$	Magnesium ions
MIC	Minimum Inhibitory Concentration

min	Minute
mL	Millilitre
mm	Millimetre
Mtb	*Mycobacterium tuberculosis*
MTBC	*Mycobacterium tuberculosis* complex
MTP	*Mycobacterium tuberculosis* curli pili
Rv3218 knockdown	*Rv3218*-knockdown strain
NAD	Nicotinamide Adenine Dinucleotide
NADP	Nicotinamide Adenine Dinucleotide Phosphate
NCBI	National Centre for Biotech Information
Nm	Nanometres
OADC	Oleic acid-albumin-dextrose-catalase
OD	Optical Density
OM	Outer Membrane
PA	Phosphatidic Acid
PAHO	Pan American Health Organization
PAM	Protospacer Adjacent Motif
PBS	Phosphate Buffered Saline
PCR	Polymerase Chain Reaction
Pfam	Protein families
PLG	Poly-L-Glutamine
PM	Plasma Membrane
PZA	Pyrazinamide
QC	Quality control

RD	Research and Development
RIF	Rifampicin
RNA	Ribonucleic acid
rpm	Rotations Per Minute
RR	Rifampicin Resistant
RT-qPCR	Reverse Transcription Quantitative Polymerase Chain Reaction
s	second
SA	South Africa
sgRNA	Single-guide RNA
TA	Toxin-Antitoxin
TB	Tuberculosis
TetR	Tetracycline Repressor
tRNA	transfer RNA
µL	Microlitre
µm	Micrometre
V	Volts
v/v	Volume/ volume
WHO	World Health Organisation
WT	Wild-type
XDR	Extensively drug-resistant
w/v	weight/volume

ABSTRACT

Tuberculosis (TB), caused by *Mycobacterium tuberculosis*, is a primordial affliction that continues to torment humankind since its known history and prehistory. TB is among the major causes of ill-health and death in the world with an estimated 1.8 million cases of death recorded yearly. The situation is worsened by the emergence of the strains of TB that are regarded as resistant. Recently, *Mycobacterium bovis bacillus* Calmette-Guerin (BCG), has been the only available vaccine for TB. An intense understanding of *Mtb'*s biology, should reveal new perceptions that can lead to the improved treatment, diagnostics, vaccines and highly needed control measures. Throughout infection, *Mtb* produces some proteins into the host environment to play critical role in pathogen host interactions. Close to half of the *Mtb* genome consists of genes with unknown functions. Among those genes is *Rv3218* gene which was identified in the study by Chiliza *et al.,* 2019. The *Rv3218* gene is hypothesised to have a Diacylglycerol kinase activity. This study aimed at characterising the function of *Rv3218* gene in *Mtb* with the purpose of coming up with ideas of how that can be used in the development of more effective and convenient diagnostic tools, therapeutics, or the total elimination of TB. There is a vast amount of molecular techniques that are currently used to characterise unknown genes. Here we employed a CRISPRi dCas9 system for the silencing of the *Rv3218* gene in *Mtb*. We also used a number of Bioinformatics tools for *in silico* analysis of the gene and construction of all relevant primers necessary for this molecular cloning. The *Rv3218* knockdown repressed by Anhydrotetracycline (ATc) was constructed for assaying the effect of this gene silencing compared to the *MtbH37Rv* wild type. We then conducted growth curves and MICs (Minimum Inhibitory Concentrations) to check if this gene has an impact on antimicrobial susceptibility and growth of *Mtb*. We also tested its activity as a diacylglycerol kinase via osmolarity assay as it is said that dgk mutants do not grow well on nutrient media of low osmolarity. On bioinformatics analysis, we found that the gene has cell wall and transcription regulatory functions and possesses a similar structure as diacylglycerol kinase. However, the *in vitro* analysis was contradictory to these findings. We found that the *Rv3218* gene has no impact on the growth of *Mtb* and it's susceptibly to the antimicrobial drugs that were used in this study. On the osmolarity assay, there was no observable difference between the growth of the wild type and the knockdown strain in all the concentrations of osmolarity. Judging from these findings, we then concluded that this gene does not function as a diacylglycerol kinase. We then suggested that, more advanced experimental studies still need to be conducted in order to confirm this hypothesis as we were unable to do them due to the short time frame for this study.

Chapter 1: Literature Review

1.1 Introduction to Tuberculosis Epidemiology

Tuberculosis (TB) is a contagious disease that is the main cause of sickness and one of the leading cause of death throughout the world (WHO, 2021; WHO 2022). Tuberculosis has been the main source of death from a single infectious agent, ranking slightly above Human Immunodeficiency Virus and Acquired Immunodeficiency Syndrome (HIV/AIDS) before the onset of the coronavirus (COVID-19) pandemic (WHO, 2021). According to forecasts from the Pan American Health Organization for 2022, close to 28,000 people get sick with this avoidable and treatable disease every day, and over 4100 people die from TB (POHA, 2022). Since the year 2000, it is projected that 66 million lives have been spared due to global efforts to combat tuberculosis (POHA, 2022). However, years of gains in the struggle to end TB have been reversed by the COVID-19 pandemic, with death cases of 2020 returning to the level of 2017 (WHO, 2021; POHA, 2022) and the first observed year-to-year rise of 5.6 % since the year 2005 (WHO, 2021). The largest global decline was noticed in the reported number of people receiving a new TB diagnosis (WHO, 2021; WHO, 2022). This dropped to 5.8 million in 2020 from a peak of 7.1 million in 2019, returning to the level last seen in 2012 (WHO, 2022). A modest rebound occurred in 2021, reaching 6.4 million (the level of 2016–2017) (WHO, 2022). The biggest challenge was that, finances and all the essential resources had been shifted to COVID-19 management, testing, and diagnostic capabilities since the pandemic's emergence (WHO, 2022).

Tuberculosis has had a massive impact in resource poor countries. Lack of rapid diagnostic tests and effectual drugs pose a greater challenge in the eradication of TB. Two thirds of the incidence cases worldwide were reported in 8 of the top 30 high TB countries: India (26 %), Indonesia (8.5 %), China (8.4 %), Philippines (6 %), Pakistan (5.7 %), Nigeria (4.4 %), Bangladesh (3.7 %), and South Africa (3.7%) (WHO, 2020). South East Asia (44%), Africa (25 %) and the Western Pacific (18 %) had the most incident cases (WHO, 2020). In South Africa, the incidence of TB was predicted to be 615 cases per 100,000 people in 2019, ranging from 427 to 835 cases per 100,000 people (Dlatu *et al*, 2022). This is in spite of the fact that

since the year 2009, the incidence of TB has been sharply declining in South Africa (Dlatu *et al*, 2022).

Globally, 10 million people contracted the illness in 2021, and 8.2% of those were HIV positive. The global TB burden is growing as a result of rising treatment resistance, HIV co-infection, and a lack of efficient vaccines. South Africa is included on the top 3 lists created by the WHO to identify nations with a high prevalence of TB, TB-HIV co-infection, and multidrug-resistant TB (MDR-TB). Close to 7 700 of the 227 224 cases of TB that were recorded in South Africa in 2021 were drug-resistant strains (WHO, 2022). In 2021, TB claimed the lives of almost 1.3 million persons who were HIV-negative and 0.3 million people who were HIV-positive (WHO, 2022). In sub- Saharan Africa, the TB epidemic is spreading and HIV infection is rising (UNAIDS, 2017; Mohammed *et al.*, 2018). Close to 72 % of the 10 million new cases of TB recorded in 2021 were among people living with HIV (Figure 1.1) (WHO, 2022). In 2021 alone, HIV-TB co-infection caused 208 000 fatalities (WHO, 2022). Human immune deficiency virus weakens a patient's immune system, which makes them more vulnerable to TB. People living with HIV have an increased risk of contracting TB 18 times greater than that of HIV-negative people (WHO, 2022). The global estimation of the prevalence of HIV-TB co-infection in 2022 is illustrated in **figure 1.1** below:

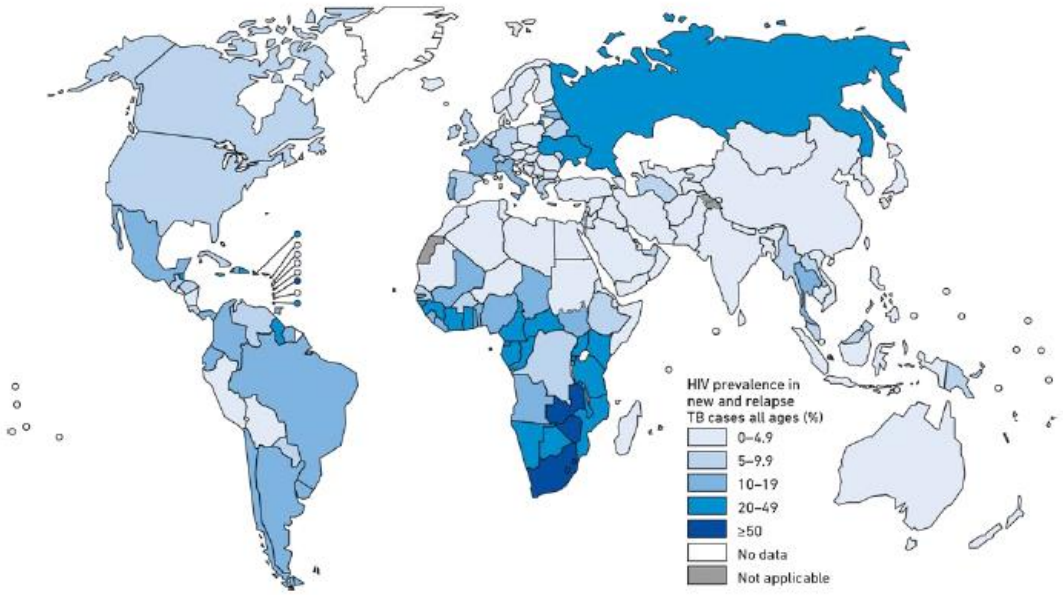

Figure 1.1: A worldwide estimate of the prevalence of HIV-TB co-infection in 2022 (WHO, 2022). The estimation is amongst new and relapse TB cases for all ages reported in percentage (%).

1.2. The structure and Morphology of *Mtb*

Mycobacterium tuberculosis is a facultative intracellular pathogen (Kalscheuer *et al.*, 2019), gram- positive and acid fast with a G+C content of 60 % to 70% (Cook *et al.*, 2009). They are irregular rods with a diameter of 0.3-0.5 µm, and are aerobic with variable lengths (Cook *et al.*, 2009). The major components of the *Mtb's* cell wall are the mycolic acids (Cook *et al.*, 2009). The morphology, physiology and behaviour of *Mtb* and other mycobacteria is mainly controlled by the mycobacterial cell envelope which mainly comprises of highly structured sugars and lipids (Chiaradia *et al.*, 2017). This cell envelope is critical for the physiology of the bacteria because it harbours a lot of essential processes which include receptor adhesion, bacterial defence mechanism against hostile environments, transportation of solutes and proteins, and mechanical resistance (Chiaradia *et al.*, 2017). About 40 % of the cell dry mass is mainly lipids, although this figure may differ depending on the type of isolates, species and growth conditions (Jackson, 2014). The complex structuring of the components of the *Mtb's* cell envelope (illustrated in figure 1.2) elucidates some of the *Mtb* cell wall's low permeability for many drugs (Kalscheuer *et al.*, 2019; Maitra *et al.*, 2019). This limited permeability may be the major cause of *Mtb's* antimicrobial resistance and pathogenesis (Maitra *et al*, 2019). The mycobacterial cell envelope comprises of four layers: (i) the plasma membrane or inner membrane (IM), (ii) the peptidoglycan-arabinogalactan complex (AGP), (iii) an asymmetrical outer membrane (OM) or'mycomembrane,' which is attached covalently to AGP through mycolic acids, and (iv) the outermost capsule (Kalscheuer *et al.*, 2019).

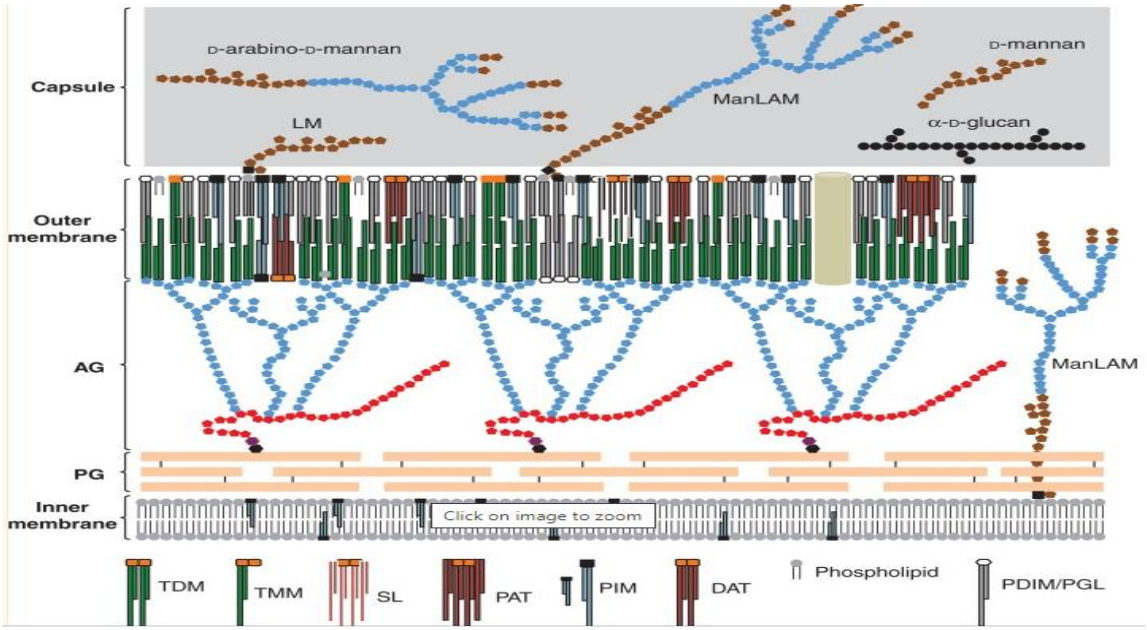

Figure 1.2: Schematic representation of the *Mtb* cell envelope. (Jackson, 2014). Blue symbols represent arabinose residues, red represent galactose residues, brown represents mannose residues, and black circles represent glucose, dark green represent mycolic acids.

One of the main constituents of the pathogenic mycobacterial cell was is the poly-L-glutamine/glutamate (PLG) which is a polymer that is synthesized by the enzyme glutamine synthetase (GS) (Garg *et al.*, 2014). This enzyme's direct involvement in the production of the polymer PLG was confirmed when the *glnA1* gene of *Mycobacterium bovis* was expressed ectopically in the *Mycobacterium smegmatis* saprophytic strain, which does not have PLG in the cell wall, which then produced it in large numbers (Garg *et al.*, 2014). The *glnA1* gene is very important for bacterial growth and survival and its disruption can lead to changes in the characteristics of the cell wall and a decrease in the production of PLG (Garg *et al.*, 2014).

1.2.1 The inner membrane (Plasma Membrane)

The *Mycobacterium tuberculosis* innermost membrane, which is the plasma membrane, appears to be almost similar to that of other bacteria excepts for the fact that *Mtb'*s plasma membrane consists of the mycobacterium specific components which are lipoglycans, (lipo)-proteins and (glyco)-lipids (Angala *et al.*, 2014; Jackson, 2014). Among the lipoglycans that are present in the *Mtb'*s plasma membrane, decaprenyl phosphate (Dec-P) functions as a transporter of activated sugars during the production of crucial cell envelope polymers which include PG, AG, LM, and ManLAM (Jackson, 2014). This simply means that the lipids of the *Mtb's* plasma membrane have intrinsic roles in the physiological processes such as DNA

replication, synthesis of ATP, transportation of electrons and biosynthesis of other cell envelope components, also functions as the selective permeability bearer around the cell (Jackson, 2014).

1.2.2 The peptidoglycan–arabinogalactan complex (AGP)

Arabinogalactan (AG) is the polysaccharide that is formed of arabinose and galactose subunits (Niederweis *et al.*, 2010) that covalently joins the mycolates to the peptidoglycan through a distinctive linker unit at its reducing end and is also found below the mycolic acid domain of the mycobacterial cell wall (Dover *et al.*, 2004). Mycolic acids are unusually lengthy fatty acids that account for 30 % to 40 % of the mass of the cell envelope (Niederweis *et al.*, 2010). Peptidoglycan (PG) is a composite macromolecular structure instated outside of almost all eubacterial plasma membranes (Alderwick *et al.*, 2015). The peptidoglycan mesh-like positioning provides rigidity, allowing the cell to resist osmotic pressure while maintaining cell intergrity and shape (Alderwick *et al.*, 2015).

1.2.3. The Capsule

Mycobacterium tuberculosis capsules are made up of neutral polysaccharides, proteins, and trace amounts of lipids (Kalscheuer *et al.*, 2019). Polysaccharides were discovered to be the paramount capsular constituents in mycobacterial species that are slow growers whereas proteins appear to be the main constituents in fast-growing mycobacterial species such as *M. smegmatis* (Kalscheuer *et al.*, 2019). The cell envelope outer compartments, also known as the 'capsule, is made up of a polysaccharide, protein, and lipid mixture (Daffe and Etienne, 1999). They are regarded as capsular not in the sense that its components are not non-covalently bound to the cell wall, but because its outermost compartments function and act like the capsule (Daffe and Etienne, 1999). A study by Daffe and Etienne argued that the essense of the capsule may be much more bacterial than that of host origin. They also stated that what seemed to be a capsule could be noted in a variety of pathogenic mycobacteria published images as an Electron Transparent Zone (ETZ) exterior the bacterial wall but enclosed by the phagosomal membrane and frequently by host origin material (Daffe and Etienne, 1999).

1.3 Mycobacterium tuberculosis Pathogenesis

Tuberculosis is mainly disseminated via aerosolized droplets, which are 1-5 µm in diameter (Ahmad, 2011), containing an infectious *Mtb* from the cough of an individual infected with

lung *Mtb*, normally called an Active Pulmonary Disease (Glickman and Jacobs, 2001; Ahmad, 2011; Sia *et al.,* 2011). There are several factors that determine the risk of infection. These include the size of the inhaled bacilli, the source of infection, distance from contact, and the immunity status of the possible host (Ahmad, 2011).

1.3.1 Latent TB

After inhalation, the *Mtb* bacilli embed themselves onto the terminal air spaces of the lung from where they replicate within the alveolar macrophages (Glickman and Jacobs, 2001). Macrophages are critical white blood cells that help in the elimination of foreign particles and initiating an immune response. In that way, since *Mtb* is a foreign substance, it is easily phagocytized by the alveolar macrophages and can easily be killed due to the initiated immune response (Delogu *et al*., 2013). However, it can be difficult for the alveolar macrophages to completely eliminate *Mtb* because of its various virulence factors which include the high mycolic acid content found in the *Mtb's* outer capsule, and the cord factors that can impair the macrophages (Jilani *et al.,* 2022). Once phagocytized by the host macrophages, *Mtb* inhabits the membrane-bound vacuole from where it enhances its own intracellular survival mechanism by deliberately modifying the maturation of this phagosomal compartment (Glickman and Jacobs, 2001; Jilani *et al.,* 2022). If by any chance the bacilli survive this first survival mode, it starts replication within the macrophages from where it starts disseminating to the nearest cells inclusive of epithelial and endothelial cells, reaching a high bacterial burden (Delogu et al, 2013). From there, *Mtb* spreads to other organs of the body via the lymphatics where it can infect other cells through haematogenous dissemination (Delogu *et al.,* 2013). Once the adaptative immune response starts, a cellular infiltrate that later resembles a typical structure of a granuloma is formed. This granuloma is formed by the relocation of the *Mtb* bacilli to the site of earliest infection of neutrophils, lymphocytes and other immune cells, which are attracted by the chemokines and cytokines produced by the macrophages in the lungs (Delogu *et al.,* 2013; Jilani *et al.,* 2022). At this stage, the *Mtb* bacilli remain encapsulated inside the granuloma, which is prior covered by the fibrotic components, and protected by the host immune response (Smith, 2003; Delogu *et al.,* 2013). In this stage, a lesion called the Ghon complex is formed and it is thought to be the refuge for the *Mtb* bacilli. Inside the Ghon complex, the *Mtb* bacilli becomes dormant in a non-metabolically active state and can remain that way for years and even for eternity (Smith, 2003; Delogu *et al,* 2013). This is called the latent infection, where *Mtb* remains non-functional, inactive, asymptomatic and non-

contagious. In individuals with a sturdy immunity, the infection may remain arrested permanently (Smith, 2003).

1.3.2 Active TB

If the individual becomes immune-compromised by Human Immunodeficiency Virus (HIV), aging, lack of nutrition, drugs and other factors, the Active TB disease may develop (Smith, 2003). In this case, the granuloma centre, which was healed during latent infections, becomes precipitated by an unknown process and then acts as a rich medium for the newly resuscitated *Mtb* to replicate in an unmanageable way (Smith, 2003). The live *Mtb* can now move from the granuloma and disseminate to the lungs from where they form an active pulmonary TB, and to other organs through the lymphatic systems and the blood where it causes Extrapulmonary TB (Smith, 2003). At this stage, the individual becomes highly contagious and requires urgent need of antibiotic therapy (Smith, 2003). The process for the pathogenesis of the *Mtb* bacilli is clearly illustrated in figure 1.3 bellow:

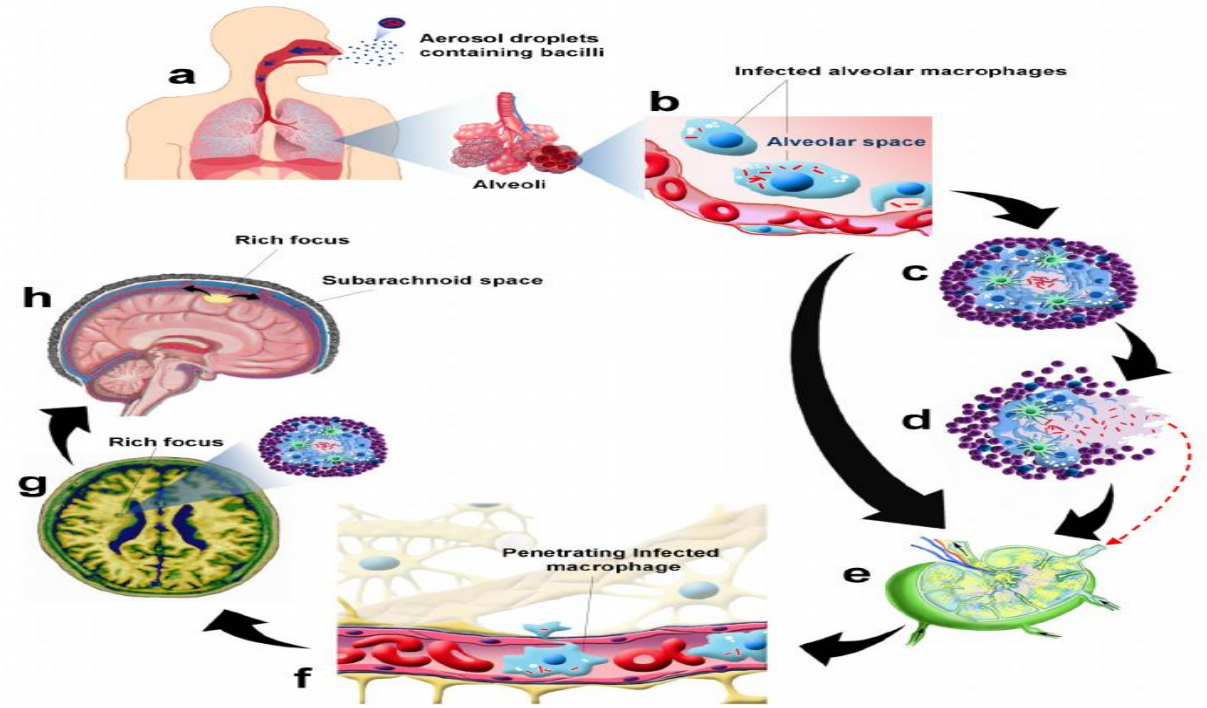

Figure 1.3: A diagrammatic illustration of *Mycobacterium tuberculosis* pathogenesis (Smith, 2003).

1.4 Development of Tuberculosis Vaccines and Drugs

1.4.1. Vaccines

On the present days, the development of novel and up-to-date vaccines is the main stream of Research and Development (RD) in the attempts to curb TB infection and tackle the dissemination of MDR/XDR-TB (Ahsan, 2015). Currently, the Bacille Calmette-Guérin (BCG), which was developed in 1921, is the only available, licensed vaccine against TB (Scriba *et al*, 2020; Behr *et a.l*, 1999). The major drawback of the BCG vaccine is that it is not reliable against pulmonary TB in adults and adolescents (Roy *et al.*, 2014). These age groups are the leading transmitters of TB making them a priority target population for the development of TB vaccines (Scriba *et al.*, 2020). Currently, there are 12 candidate vaccines that are being tested in clinical trials (Tammeris *et al.*, 2013; Gonzalo-Asensio *et al.*, 2017).

A variety of candidate vaccines under development are grouped into different classifications namely; the live-attenuated whole-cell vaccine, the inactivated whole-cell vaccine, viral-vectored vaccine, and adjuvanted protein vaccines (Gonzalo-Asensio *et al.*, 2017; WHO, 2020; Gopalaswamy and Subbian, 2022). The live attenuated whole-cell vaccines involves the use of a whole *Mtb* in modified and weakened state (Whitlow *et al.*, 2020). The examples of these vaccines include the recombinant BCG VPM1002 which is known to be the most progressive live-attenuated vaccine in clinical development (Gonzalo-Asensio *et al.*, 2017). The rBCG VPM1002 entered the efficacy experiments directed at averting TB infection in newborns with and without HIV infection (Gonzalo-Asensio *et al.*, 2017). The other live-attenuated whole-cell vaccine is the MTBVAC which was the first and distinctive live attenuated vaccine accredited into clinical trials in the year 2012 (Gonzalo-Asensio *et al.*, 2017; Pérez *et al*, 2020). The MTBVAC is unique in the sense that it was the first developed vaccine that involves the attenuation of the genetically modified form of the human pathogen *Mtb* and it is used for both infants and adults (Pérez *et al.*, 2020; Tarancon *et al*, 2020). The inactivated whole-cell vaccines were developed to boost the efficacy of BCG (von Reyn *et al.*, 2017) and the example includes the SRL 172 whole-cell vaccine acquired from a non-tuberculous mycobacterium (Kaufmann *et al.*, 2016; von Reyn *et al.*, 2017). Another example of inactivated vaccines is the inactivated RUTI vaccine, which consists of disintegrated and detoxified *Mtb* cells in

liposomes (Whitlow *et al.*, 2020). Inactivated vaccines are mostly regarded as being the safest in comparisons with the live vaccines particularly since they do not contain any infectious agents (Whitlow *et al.*, 2020). The adjuvant protein subunit vaccines also fall under safe vaccines since they only consist of determined parts or subunits of the pathogen. The most commonly used proteins for this type of vaccine development include ESAT6, MPT64, Ag85B, and Ag85A (Whitlow *et al.*, 2020). The recombinant viral-vectored vaccines are known for their ability to induce vigorous immune responses by imitating the actions of the invading pathogens leading to the emergence of the long-lasting immune memory (Hu *et al.*, 2022). The most modern recombinant vaccines include MVA85A, ChAdOx1.85A, AdHu35, and AERAS-402 (Stylianou *et al.*, 2015; Hu *et al*., 2022).

The goal for TB vaccines development is to reduce the spread of the disease and to protect all the individuals that are at a greater risk of being infected, hospitalised, and potentially dying from this infectious disease. Since the only licenced vaccine against TB offers limited protection and is only effective against pulmonary TB in new-born babies, there is an urgent need for the development of novel vaccines that will be highly effectual against TB in all generations; infants, adolescents and adults in order to end TB, combat its spread, and to prevent its progression to drug resistance (WHO, 2022).

1.4.2 Tuberculosis Drugs

The correct diagnosis and medical treatment of tuberculosis represent a keystone in the management and control of Tuberculosis (Sotgiu *et al.*, 2015). Antibiotic treatment which is critical for the depletion of bacterial burden in the lungs, can be useful in the reduction of probability of transmission, along with other public health measures, such as isolation and cough etiquette (Sotgiu *et al.*, 2015). Tuberculosis medications are categorized into two main groups; the first line and the second line of drugs (Sia *et al.*, 2011). The first line drugs are the most commonly used drugs and they include Isoniazid (INH) in combination with rifampin (RIF), pyrazinamide (PZA) and ethambutol (EMB) (Sia *et al.*, 2011; Bendre *et al.*, 2021; American Lung Association, 2020). These drugs are usually used to treat active pulmonary TB that is not drug-resistant (Bendre *et al.*, 2021). Bedaquiline (BDQ), Aminosalicylate, Kanamycin, Cycloserine, Ethionamide, Amikacin, Capreomycin, Thiacetazone, and Fluoroquinolones fall under the second-line of drugs category and are mainly used in the treatment of M/XDT TB (Bendre *et al.*, 2021; Sia *et al.*, 2011; Joshi, 2011).

Individuals that are infected with the active TB usually undergo what is called anti-tubercular chemotherapy which is a two-phased therapy consisting of a first rigorous phase with three or more drugs, and a second continuation phase with just two to three drugs (Joshi, 2011). The short course chemotherapy, which is the first phase, usually takes about two months, and the continuation phase takes about four months (Unissa and Hanna, 2017). The initial intensive phase regimen includes all four of the drugs falling under first-line of drugs (RIF, INH, PZA and EMB) (Unissa and Hanna, 2017). The continuation phase of the chemotherapy encompasses a choice of a variety of options including INH and RIF for four months, or alternatively, INH and EMB or thiacetazone for six months, with INH being the most effective drug (Joshi, 2011; Unissa and Hanna, 2017).

1.4.2.1 Isoniazid (INH)

Since its first discovery in the 1950s, Isoniazid (INH) remains a centrepiece of anti-tubercula chemotherapy for active TB (Diacon *et al.*, 2020; Timmins and Deretic, 2006). Isoniazid is one of the main antibiotics that are rapidly bactericidal both *in vitro* and *in vivo* for the treatment of *Mtb* infections (O'Connor and Brady, 2022; Diacon *et al.*, 2020). Isoniazid's mode of actions includes its initial entry to mycobacterial cell through passive diffusion where it acts as a prodrug that is activated by the by the mycobacterial enzyme called the KatG (Timmins and Deretic, 2006). This is done because INH on its own is not toxic to the bacterial cell (Timmins and Deretic, 2006). The enzyme KatG, is a catalase-peroxidase that has many other activities including peroxynitritase and NADH oxidase (Timmins and Deretic, 2006). This is a process that formulates several radicals and adducts that prevent the mycobacterium's production of mycolic acids that form its cell wall (O'Connor and Brady, 2022). This activity is the main reason why INH is regarded as a powerful antibacterial agent (O'Connor and Brady, 2022). However, as powerful as INH is, it can also be prone to mutations via the disruption of the KatG which may lead to resistance in INH therapy (O'Connor and Brady, 2022). This resistance may only develop when INH monotherapy is used for the treatment (O'Connor and Brady, 2022).

1.4.2.2 Rifampin

Rifampin, a semisynthetic derivative of rifamycin, is an antibacterial agent used to prevent and treat many gram-positive cocci, *Mycobacteria* and other gram-negative bacteria including *Neisseria meningitides* (Suresh *et al.*, 2022; Unissa and Hanna, 2017). Due to the high sterilization function of RIF; which is its ability to kill persistent or metabolically dormant *Mtb*,

it has formed a cornerstone of the short course chemotherapy in conjunction with INH and PZA (Unissa and Hanna, 2017). Clinically, RIF is used for pathogens whose identities are known and their drug susceptibility has been determined (Suresh *et al.,* 2022). Its mechanism of action includes the production of bactericidal antimicrobial activity either by sterically blocking the path of the elongating RNA at the 5′ end or by decreasing the affinity of the RNA polymerase for short RNA transcripts all leading to the inhibition of the DNA dependent RNA polymerase activity (Suresh *et al.,* 2022). This simply means that the main function of RIF is to halt further RNA synthesis of *Mtb*, by inhibiting the microbial RNA polymerase activity (Pang *et al.,* 2013; Suresh *et al.,* 2022).

1.4.2.3 Pyrazinamide (PZA)

Since its clinical use in 1952, the mode of action of Pyrazinamide (PZA) has been mysterious, contradictory, and unconventional (Zhang *et al.,* 2013). Pyrazinamide is different from the other commonly used antibiotics that function against the growing bacteria and no or little activity for non-growing persisters (Zhang *et al.,* 2013). Even though PZA has a powerful sterilizing activity *in vivo,* it is said that it has no activity *in vitro* under normal culture conditions at neutral pH, but is active only at an acid pH (from pH 5.5 to pH 6) as seen in the phagosomal compartments in *vitro* (Whitfield *et al.,* 2015; Zhang *et al.,* 2013). For PZA to be toxic to *Mtb* under acidic conditions first requires its conversion to its functional form called pyrazinoic acid with the assistance of the enzyme pyrazinamidase encoded by the *pnc*A gene (Che *et al.,* 2021). Pyrazinamide is also known for its excellent ability to kill non-replicating persisters that other TB drugs cannot kill, which makes it an important drug to be included in any drug combination for treating drug resistant TB (Zhang *et al.,* 2013).

1.5 *Mycobacterium tuberculosis* Drug Resistance

Mycobacterium tuberculosis drug resistance is a biological incident that has been perceived since the discovery of streptomycin, the first ant-TB drug (Seung *et al.,* 2015). Tuberculosis therapy and the effectual disease control strategies are challenged by the emergence of multidrug resistant (MDR) and extensively drug resistant (XDR) TB, and now poses a major threat to global public health (Palomino and Martin, 2014*;* Seung *et al.,* 2015; Singh *et al.,* 2019). Drug resistance in TB is mainly effectuated exclusively by chromosomal mutations which interfere with the drug target itself or the bacterial enzymes that activate pro-drugs

(Unissa and Hanna, 2017). Multidrug resistant TB is caused by the resistance of the *Mtb* strains to at least two of the main drugs of TB therapy, which are INH and RIF (Palomino and Martin, 2014). The Centre for Disease Control (CDC) state that many factors contribute to the resistance to anti-TB drugs. These factors include the misuse and mismanagement of these drugs, for instance, when wrong treatment is prescribed by health-care workers, when patients do not complete their full treatment course, the wrong prescribed time and dose for taking the treatment, poor quality of drugs, and when the supply of drugs is not always available (CDC, 2016). Two broad categories of *Mtb* drug-resistance mechanisms have been reported and they are intrinsic drug resistance and acquired drug resistance. The intrinsic resistance is where the *Mtb* is not only resistant to the already introduced drugs but also to the ones that are newly introduced (Swain *et al.,* 2020). The acquired drug resistance is inaugurated due to the origin of chromosomal mutations under selective pressure (Swain *et al.,* 2020). These chromosomal mutations may include the mutations on the peroxide enzyme (KatG) associated with resistance to INH, and also chromosomal mutations in the quinolone resistance-determining region in position 90 to 94 of gyrA associated with resistance to fluoroquinolone (Palomino and Martin, 2014).

Drug resistance in *Mtb* progresses through a variety of procedures which include clonal interference, epistasis, cell envelop impermeability, efflux pump, drug degradation and modification, compensatory evolution, target mimicry and phenotypic drug tolerance (Al-Saeedi and Al-Hajoj, 2017; Rojas *et al.*, 2019). The drug-resistant TB advancement can be regulated by ensuring swift and suitable diagnosis, accurate and prudent utilization of drugs for therapy, sufficient infection management in the facilities of TB treatment, adherence of patients to drug processes and social perceptions on TB management (Singh *et al.,* 2019; Dartois and Rubin, 2022). Better interventions can have a very important and considerable result on the capacity to lessen the mortality and morbidity related to the disease and to halt further spread of the disease (Dartois and Rubin, 2022). These interventions could also be improved by firstly understanding the biochemical, molecular and genetic core of resistance in order to be able to draw up novel therapeutic strategies and fight drug resistance (Singh *et al.,* 2019).

1.6 *Mycobacterium tuberculosis* genome and hypothetical proteins

1.6.1 The Mtb genome

Since its first isolation in 1905, the *Mtb*H37Rv strain still remains the most pathogenic strain and has been extensively used worldwide in biomedical research leading to the clarification of

the metabolism, biology and evolution of this pathogen (Cole *et al.,* 1998; Loerger *et al.,* 2010; Camus *et al.,* 2002). The *Mycobacterium tuberculosis* H37Rv is made up of 4.4 million base pairs and it contains approximately 4000 genes with an average G+C content of 65.6 % (Cole, 1999; Smith, 2003; Advani *et al.,* 2019). The H37Rv strain has been widely used in laboratories because of its ability to retain its virulence since its identification (Cole *et al.,* 1998; Loerger *et al.,* 2010). Mycobacterium tuberculosis has some unique features shown by its annotation with over 200 of its genes being annotated as encoding fatty acids metabolism enzymes (Smith, 2003; Kootery and Sarojini, 2022). This large number of genes that function in fatty acids metabolism may be related to this pathogen's ability to grow in the tissues of an infected host, where the main carbon source may be the fatty acids (Smith, 2003; Loerger *et al.,* 2010).

According to Cook *et al.,* the Mycobacterium genus encompasses about a hundred of closely related species as judged by their 16sRNA sequence comparisons (Cook *et al.,* 2009). This is in relation to 50 genes encoding stable RNA species and 3294 genes encoding proteins that were identified by means of Bioinformatics (Cole *et al.,* 1999). This rapid diversification of this genus is based on the innovation of the Polymerase Chain Reaction (PCR) for DNA sequences amplification and the 16srRNA sequences recognition as phylogenetic markers (Cook *et al.,* 2009).

1.6.*2 The Hypothetical Proteins (HPs)*

A study by Muzandu and Mulder state that, in the face of a constantly growing amounts of biological data, including primary data, such as genomic sequences, and functional genomic data from high-throughput experiments, there is an insufficiency in the functional annotation for a vast amount of recently sequenced proteins (Muzandu and Mulder, 2012). Hypothetical Proteins (HPs) are proteins that are thought to be expressed from an open reading frame but do not have experimental verification of translation (Ijaq *et al.,* 2019; Yang *et al*., 2019). In many bacterial genomes, for example, about 40 % of identified proteins are classified as "uncharacterized" or "unknown" or "hypothetical" proteins, or with similar identification that it simple means that there is no functional indication for the open reading frame in question (Doerks *et al.,* 2012; Muzandu and Mulder, 2012; Raj *et al*., 2017). The hypothetical proteins have known-unknown regions whose biological properties have not been identified and no functional links that are discovered (Ijaq *et al.*, 2019).

Mycobacterium tuberculosis genome sequence is available on the National Centre for Biotechnology Information (NCBI) database and consists of 4019 genes encoding 3906

proteins (Raj *et al*., 2017; Yang *et al.*, 2019). The *Mtb* H37Rv whole genome has been sequenced for better understanding of the *Mtb* virulence and immunity (Yang *et al*., 2019). Hypothetical proteins are thought to have some crucial roles in the progression of the diseases and the survival of the pathogen in many species (Gupta *et al.*, 2016; Yang *et al.*, 2019). A few of these hypothetical proteins such as the *Rv0079* and *Rv3873*, have been studied experimentally and characterized. The *Rv0079* was discovered to be a DosR regulon that prevents protein synthesis and interacts with TLR2 to elevate cytokine secretion (Mishra, 2009; Yang *et al.*, 2019). The *Rv3873* was discovered as being a member of the protein family that is essential for the *Mtb's* endurance in different environmental conditions (Daugelat *et al.*, 2003; Yang *et al.*, 2019). These results prove that hypothetical proteins can have critical functions in the survival of *Mtb*, even though their functions are still unclear (Yang *et al*., 2019).

Several bioinformatics tools were utilized for the forecast and comprehension of these hypothetical proteins (Raj *et al.*, 2017). Only 250 of the *Mtb's* hypothetical proteins were analysed using several bioinformatics web tools including Basic Local Alignment Search Tool (BLAST), INTERPROSCAN, and Protein Families (PFAM) database to name a few. However, more work and research still needs to be conducted for the analysis of the function of 1055 uncharacterized proteins that were isolated from the *Mtb's* H37Rv strain (Raj *et al*., 2017).

Proteins with unknown functions account for roughly half of the *Mtb* genome (Muzandu and Mulder, 2012). This big number of uncharacterized proteins limits the potential to utilize these data (Muzandu and Mulder, 2012). One of the vital duties in the post genomic era is genome annotation, where functions to gene products are allocated according to amino acid sequences (Muzandu and Mulder, 2012). The biological examination of organisms has advanced from a single gene approach to a whole genome focus, allowing a chance to explore the genes inside their context in a cell (Muzandu and Mulder, 2012).

1.7. The *Rv3218* gene, a hypothetical Diacylglycerol Kinase

According to Mycobrowser database, the *Rv3218* gene is a conserved hypothetical protein, also labelled as Non-essential gene. *Rv3218* gene was identified during a study conducted by Chiliza *et al*., 2019. Like other hypothetical proteins, the *Rv3218* gene may have some crucial

roles in the survival of the pathogen and the progression of the diseases caused by *Mtb*. A deeper understanding of this gene might give insights on the development of novel vaccines and other crucial TB diagnostic tools. It is thought to be bound in the membrane of *Mtb* H37Rv and is hypothesised to have a Diacylglycerol kinase activity. Diacylglycerol kinase (DGK) is the enzyme which phosphorylates diacylglycerol (DG) using Adenosine triphosphate (ATP) as a source of the phosphate resulting in the production of phosphatidic acid (PA) (Shirai and Saito, 2014). Diacylglycerols and Phosphatidic acids are deep-rooted second messengers (Giusto *et al,* 2010; Sakane *et al.*, 2020) and are both very critical signaling molecules (Shirai and Saito, 2014; Eichmann and Lass, 2015). Diacylglycerol kinases serve as regulators of the balance between DG and PA since they are DG consumers and PA generators (Sakane *et al.*, 2020). Diacylglycerol controls the activity and localization of a number of proteins such as chimerins, protein kinase C (PKC), Unc-13, and Ras guanyl nucleotide-releasing protein (RasGRP) (Shirai and Saito, 2014). Phosphatidic acids on the other hand activate a number of enzymes including phosphatidylinositol 4-phosphate 5-kinase, mammalian target of rapamycin (mTOR), and atypical isoforms of PKC (Shirai and Saito, 2014). In that way, DGK is known to be a main enzyme essential for the regulation of a number of cellular responses by controlling the balance of the two lipid messengers (Shirai and Saito, 2014).

A study by Van Horn and Sanders state that Diacylglycerol kinase (DAGK) activity was initially discovered in *Escherichia coli* (*E.Coli*) by Pieringer and Kunnes in 1965, then Chang and Kennedy demonstrated that DAGK is not frequently the primary source of PA, which is essential for the route of *de novo* glycerophospholipid formation. Rather, successive acylation of 3-phosphoglycerol typically produces this pool of PA. After locating the *dgkA* gene that codes for DAGK in 1978, Raetz and Newman used genetic and biochemical research to demonstrate that one of DAGK's primary roles in *E.coli* is to engage in the membrane-derived oligosaccharide (MDO) cycle (Figure 1.4) (Van Horn and Sanders, 2012; Möbius *et al*., 2019). The MDO pathway includes conveying phosphoglycerol from the phosphatidylglycerol (PG) in the exterior leaflet of the plasma membrane (Van Horn and Sanders, 2012). This process creates a diacylglycerol which is in turn phosphorylated by DAGK right after it crosses the plasma membrane to reach the innermost leaflet (Van Horn and Sanders, 2012). This means that DAGK acts as a converter of a lipid (DAG) into a non-toxic phosphatidic acid (PA), which is the central intermediate in the biosynthesis of glycerophospholipids in bacteria (Möbius *et al*., 2019).

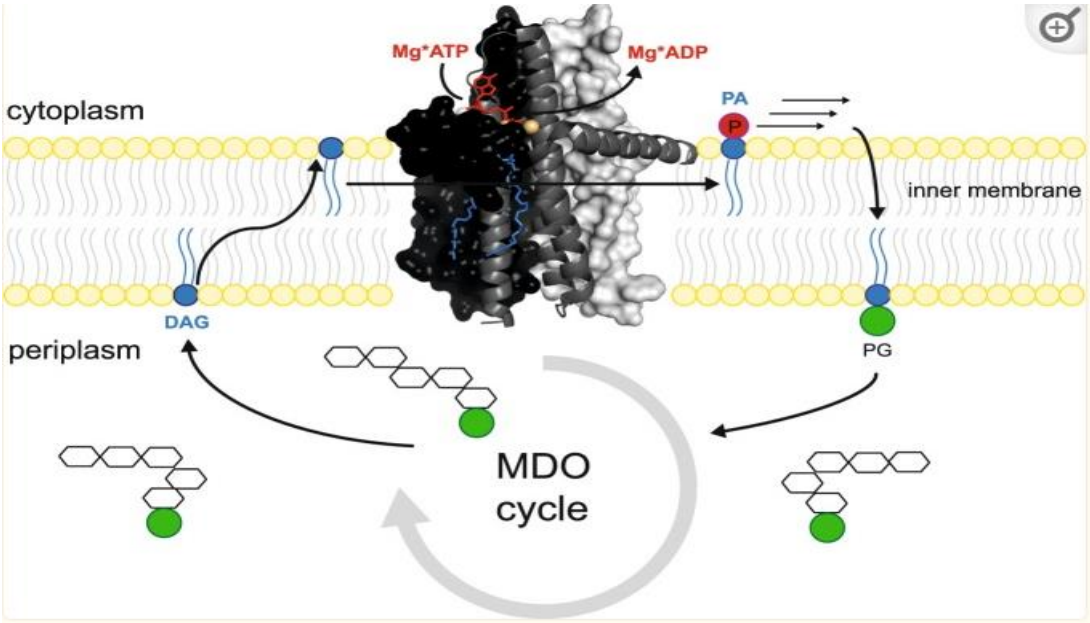

Figure 1.4: Physiological role of diacylglycerol kinase in the membrane-derived oligosaccharide (MDO) cycle of bacteria (Möbius *et al.*, 2019).

In the beginning of the 1980s, it is stated that the *dgkA* gene and the neighbouring DNA were sequenced and it was found that trans-acting mutations in a locus called the *dgkR* can augment the transcription of this gene (Van Horn and Sanders, 2012). The *dgkA* gene was also noted to be situated closer to the *plsB* gene which is thought to encode the 3-phosphoglycerol acyltransferase that functions in the commencement of the phospholipid formation pathway in *E. Coli* including the PA as a vital intermediate (Van Horn and Sanders, 2012).

1.8. The Phosphatidic Acid (PA)

Phosphatidic Acid is the comprehensible glycerophospholipid with an ancient known function of acting as a cornerstone for the formation of a variety of categories of glycerophospholipids (Kooijman and Burger, 2009; Thakur *et al*., 2019). Bacteria can produce a puzzling number of phospholipids that have important roles in the adjustment to the environment (Yao *et al.*, 2013). Phosphatidic acid is also known to be a ubiquitous forerunner required for the formation of these molecules (Yao *et al.*, 2013). Literature also suggest that phosphatidic acids are mainly the biosynthetic result of the esterification of two fatty acids onto the two hydroxyl groups of *sn*-glycerol-3-phosphate (G3P) (Yao and Rock, 2013). Beside its function in lipid

biosynthesis, phosphatidic acid is also thought to serve as the signaling molecule that regulates a number of aspects in cell biology as well as membrane transport (Kooijman and Burger, 2009; Thakur *et al.,* 2019).

1.9. Significance of the study

Collectively, most parts of the above mentioned literature suggest that the hypothetical proteins may have some crucial roles in the survival of the pathogen and the progression of the diseases caused by many species. This means that the *Rv3218* gene which is also hypothesized to be a Diacylglycerol Kinase (DAGK) might have very important roles in *Mtb* pathogenesis and survival. However, the function and the role of this gene is yet to be studied. This study focused on the characterization of the function of the *Rv3218* gene in *Mycobacterium tuberculosis* further authenticating its potential as prospective candidates for interventions for TB therapies, diagnostics and vaccinations.

1.10. Study design

1.10.1. Aim

The aim of this study is to characterise the function of *Rv3218* gene in *Mtb* through gene silencing and investigate its role during cell growth and bacterial pathogenicity. The goal is to construct a knockdown of the *Rv3218* gene using a CRISPRi method on the *Mtb* chromosome so that the phenotypes of the mutant can be characterized and compared to wild type cells.

1.10.2. Objectives

1. To analyse and perform *insilico* cloning of the *Rv3218* gene using a variety of Bioinformatics tools such as; Mycobrowser, Pfam, Itaser, STRING, and clone manager software
2. To construct *Rv3218* knockdown mutant strains using the CRISPRi method
3. To phenotypically characterize the differences between the wild type and the *Rv3218* mutant strains following these gene specific assays:
    - Osmolarity assay
    - Minimum Inhibitory Concentration assay

Chapter 2: Materials and Methods.

2.1. Ethics Approval

The current study was approved by the Biomedical Research Ethics Committee (BREC), University of KwaZulu-Natal (BREC/00001516/2020).

2.2. Bacterial Isolates and growth conditions

Bacterial strains and plasmids that were used in this study are listed in **Table 2.1** and **2.2** respectively. Bacterial stocks were prepared for each strain on sterile nutrient broth media containing 200 mL of 100% Glycerol.

2.2.1. Growth of E.coli XL-10 ultracompetent cells

Escherichia coli XL-10 ultra-competent cells were grown on nutrient broth at 37°C overnight with shaking at 100 xg and the media was supplemented with 50 µg/mL of kanamycin. The strains were also grown on solid nutrient agar media containing the same concentrations of kanamycin and incubated at 37°C overnight.

2.2.2 Growth of Mtb strains

Mycobacterium Tuberculosis (Mtb) strains (*Mtb* H37Rv wild type and transformed *Rv3218* Knockdown) were grown in Middlebrook 7H9 liquid media supplemented with 0.5 % glycerol, 0.05 % Tween 80, Oleic Acid Albumin Dextrose Catalase (OADC) (Sigma Aldrich) and appropriate antibiotic where necessary (kanamycin) at 37 °C (herein referred to as 7H9 media) with shaking at 100 xg unless stated otherwise. Antibiotic concentrations used were as follows: Kan 25 µg/mL. Bacterial strains were also grown on Middlebrook 7H11 solid media supplemented with 0.5 % glycerol, OADC (Sigma Aldrich) and appropriate antibiotics (kanamycin) at 37 °C unless stated otherwise (herein referred to as 7H11 media).

Table 1.1. Bacterial strains used in this study

Strains	Genetic information	References
Escherichia coli XL10-Gold	*Tetr*^{r}, *endA1, recA1, relA1, lacl*^{q}*ZΔM15, gyrA96, Supe44, Hte*	(Agilent Technologies, USA)
Mtb H37Rv	A virulent *Mtb* reference strain,4.41 Mbp long, 45 tRNA genes, 4081 protein genes; 13 pseudogenes, 3 rRNA, 30 ncRNA, 2 miscRNA genes, high G+C content	(Cole *et al*., 2006)
Rv3218 KD	A derivative of *Mtb* H37Rv carrying PLJR965.*Rv3218*KD, Kan^{r}	(This study)

Tet^{r}: tetracycline resistance, *endA1*: endonuclease deficient, *recA1*: recombinant deficient, *lacl*^{q}*ZΔM15:* blue-white screening. Kan^{r}: Kanamycin resistance. Mbp: Million base pairs, tRNA: transfer RNA, rRNA: ribosomal RNA, ncRNA: non-coding RNA, G+C: guanine and cytosine.

Table 1.2. Plasmids used in this study

plasmid	Genotype	Reference
PLJR965	*Mtb* CRISPRi backbone that contains Sth1 dCas9 gene, TetR, kan^{r}	(Wong and Rock, 2021)
PLJR965.*Rv3218*KD	A derivative of PLJR965 plasmid carrying annealed oligos; kan^{r}	(This study)

2.2.3 Brief description on the strains and plasmids used in this study

The *Mtb* H37Rv is the virulent strain of *Mycobacterium tuberculosis* with a genome that is 4.41 million base pairs long. The strain has a vast amount of genes that enable its survival and

growth, these include the tRNA and rRNA genes that assist in protein synthesis, the high Guanine-Cytosine composition which makes a very strong double helix structure (Cole *et al.*, 2006).

The *Escherichia coli* XL10 Gold is the strain designed to exhibit the highest efficiency of transformation of larger plasmids and ligated DNA leading to faster growth and larger colonies. This high transformation efficiency is as a result of the Hte phenotype expressed in the strains. The XL10-Gold strain is endonuclease and recombination deficient for the improvement of the quality and standard of the DNA and the assurance of insert stability. The strain is tetracycline and chloramphenicol resistant (Kamal *et al.*, 2013).

The PLJR965 plasmid is used in the expression of the Sth1 dCas9 gene and the sgRNA from a Tetracycline Repressor (TetR)-regulated promoter. This plasmid consists of the L5 integrase which allows it to insert into the *Mtb* chromosome in the *attB* site. The Kanamycin resistance of the plasmid permits for plasmid transformants selection (Wong and Rock, 2021).

2.3 Bio-informatics analysis of proteins for *insilico* cloning

The delineation of Hypothetical Proteins (HPs) by bioinformatics is of utmost importance in the understanding and advancement of genes and proteins, with its main aim being to designate some details and data to these sequences (Silva *et al.*, 2020). One other important aspect of bioinformatics is gene annotation, which its main purpose is to associate functional elements across the sequence in a genome, thereby granting meaning to it (Salzberg, 2019). Annotation of hypothetical proteins in a genome plays an important role in comprehending the gene regulation, biological role, novel target identification, gene function and metabolic pathway analysis (Thakur *et al.*, 2020). In order to predict protein structure and to predict the gene function, bioinformatics analysis was conducted using different databases and online tools. The *Rv3218* protein and gene sequences were downloaded from Mycobrowser database (https://mycobrowser.epfl.ch). Protein domain determination was carried out using the Sanger institute Protein families (pfam) tool (http://pfam.sanger.ac.uk/). Protein structure predictions and structure-based annotations were determined using Iterative Threading ASSEmbly

Refinement (I-TASSER) (https://zhanggroup.org). Protein-protein interaction functional enrichment analysis was performed on the Search Tool for the Retrieval of Interacting Genes/Proteins (STRING) database (https://string-db.org). Primer3 and celBiol (the bio-web) software were used for the designing of Polymerase Chain Reaction (PCR) primers (https://primer3.ut.ee) (http://www.cellbiol.com), primer sets for gene of interest were designed to contain a forward and reverse complement primer pair for designing the annealing oligonucleotides. Clone manager software (CMSuite9) was used for *insilico* cloning.

2.4 Plasmid extraction

2.4.1 Bulk PLJR965 plasmid extraction using GeneJet plasmid midiprep kit

This extraction was done according to manufacturer's instructions (Thermo Fisher Scientific, SA). Briefly, 1 mL PLJR965 plasmid frozen stock was aliquoted into 50 mL of nutrient broth supplemented with 50 µg/mL of kanamycin. The PLJR965 culture was then grown overnight at 37 °C on the shaking incubator (Incubator shakers, Polychem Supplies). The cells were then harvested by centrifugation (Multifuge 3 S-R, Thermo Scientific, Germany) for 10 minutes at 5000 × *g*. The supernatant was discarded and the pellet was re-suspended in 2 mL resuspension solution supplied in the kit. A volume of 4 mL solution II was added followed by mixing. The reaction was then allowed to sit at room temperature (25 °C -/+ 5 °C) for 5 min followed by mixing with 3 mL solution III. The reaction was then incubated on ice for 10 min followed by centrifuging (Multifuge 3 S-R, Thermo Scientific, Germany) for 40 min at 4000 × g. This step was done to pellet cell debris and chromosomal DNA. The supernatant was then transferred into a 15 mL tube (supplied in the kit) by decanting. A volume of 3 mL of 96 % ethanol (Thermo Scientific) was added and mixed immediately by inverting the tube 5 to 6 times. A volume of 5.5 mL of the sample was transferred to the supplied column pre-ensemble with 15 mL collection tube (supplied in the kit). The sample was then centrifuged (Multifuge 3 S-R, Thermo Scientific, Germany) for 3 min at 2,000 × *g* in a swinging bucket rotor. The flow through was then discarded and the column was placed into the same collection tube. This step was repeated to process any remaining lysate through the purification column. A volume of 4 mL of Wash Solution I was added to the purification column followed by centrifugation (Multifuge 3 S-R, Thermo Scientific, Germany) for 2 min at 3,000 × *g* in a swinging bucket rotor. The flow through was discarded and the column was placed back into the sample

collection tube. A volume of 4 mL of Wash solution II was added to the purification column, centrifuged (Multifuge 3 S-R, Thermo Scientific, Germany) for 2 min at 3,000 × g in a swinging bucket rotor. The flow through was discarded and the column was placed back into the collection tube. The column was washed with Wash Solution II step was repeated followed by centrifugation (Multifuge 3 S-R, Thermo Scientific, Germany) for 5 min at 3,000 × g in a swinging bucket rotor to remove residual Wash solution. The collection tube containing the flow-through was discarded. The column was transferred to the fresh 15 mL (supplied in the kit) collection tube. A volume of 0.35 mL of the elution buffer was added to the centre of the purification column membrane, incubated for 2 min at room temperature (25 °C ± 5 °C) and centrifuged (Multifuge 3 S-R, Thermo Scientific, Germany) for 5 min at 3,000 × g in a swinging bucket rotor to elute plasmid DNA. The purification column was then discarded and the purified plasmid DNA was stored in -20 °C.

2.5 Restriction digest for PLJR965 plasmid

Before restrictions, the extracted plasmid was firstly quantified using a NanoDrop 2000 (Thermo Fisher Scientific, Massachusetts, USA). Restriction digests were carried out using ThermoFischer restriction digest enzymes and the reactions were carried out according to manufacturer's instructions. Briefly, 1 µg PLJR965 DNA was mixed with 2 µL 10X Tango Buffer (THermo Fisher Scientific), 20 mM Dithiothreitol (DTT) (Thermo Fisher Scientific), 1 µL Esp3I (BsmBI) (10 U/µL) (Thermo Fisher Scientific, ER0451) and 15 µL sterile distilled water. The reaction was then incubated at 37 °C for 1 hour, followed by heat inactivation at 80 °C in a heating block (Dry bath incubator, MRC) for 10 min. This reaction was carried out on 0.5 mL PCR tubes (MicroAmp reaction tubes, Thermo Fisher Scientific).

2.6 Agarose gel electrophoresis

Separation of high molecular weight DNA was accomplished by using 0.8 % agarose gel made in 1 x Sodium Borate Buffer (made from a 20 x that contained 47 g boric acid (Merck Millipore) and 8 g sodium hydroxide (Sigma-Aldrich) mixed in 1 L distilled water (Merck Millipore,). Electrophoresis was conducted in 1 x sodium borate buffer at 100 Volts (V) in electrophoresis tanks (Bio-Rad laboratories). To estimate the size of the bands, DNA molecular weight ladder (1 kb GeneRuler, Thermo Fisher Scientific) was used. Gels were visualized using G: Box

SYNGENE (Vacutec) system in conjunction with the GeneSys image acquisition software (Syngene v 1.8.0.5).

2.7 Construction of a Knockdown using the CRISPRi system

In this study, for the construction of a knockdown, the CRISPR/Cas9 system has been followed which allows for the coherent genome editing without leaving any other genomic scars. The Clustered Regularly Interspaced Short Palindromic Repeats interference (CRISPRi) is a genomic editing technology that utilizes the catalytically inactive CRISPR-associated protein (dCas9) and single guide RNA (sgRNA) to repress sequence-specific genes (Choudhary *et al*., 2015). The sgRNA molecule contains the 20-nulceotides long sequence complementary to the target DNA, fused with the trans-activating CRISPR RNA which acts as a binding scaffold for the cas9 nuclease. The Cas9 protein contains four functional domains that assist in its mode of action namely; the REC I, the Bridge helix, the RuvC and HNH domains. The REC I is the largest domain that is in charge of binding the sgRNA and the Bridge Helix domain is important for initiating cleavage activity on binding of the target DNA. The role of the HNH and the RuvC, as nuclease domains, is to cut single stranded DNA (Qi, *et al.,* 2013).

The Cas9 binds to the sgRNA and forms a protein-RNA complex. The protein-RNA complex then binds to the specific DNA targets adjacent to the Protospacer Adjacent Motifs sequence (PAM), which are used to mark proper target sites, leading to the cleavage of the target DNA as a result of the Cas9 nuclease activity by the RuvC and HNH domains (Qi *et al.*, 2013). The Protospacer Adjacent Motifs is a very short DNA sequence, usually 2-6 bpd long that follows the DNA region targeted for cleavage by the Cas9. The CRISPR/Cas9 system can be modified or altered for target gene regulation other than gene disruption. The major components of this modification is a catalytically dead cas9; termed dCas9, that lacks the endonuclease activity (Zhao *et al.*, 2017). In the case of a nuclease-deficient dCas9, which consists of two substitutions in the nuclease domains (D10A and H840A), if the target DNA sequence locates inside the Open Reading Frame, the dCas9-sgRNA-DNA complex will block the movement of the RNA polymerase from binding to the promoter leading to transcription inhibition of the target gene, thereby causing gene silencing (Zhang *et al.,* 2001). This hindrance of transcription occurs in the sgRNA base-pairing genomic locus (Peters *et al.,* 2016).

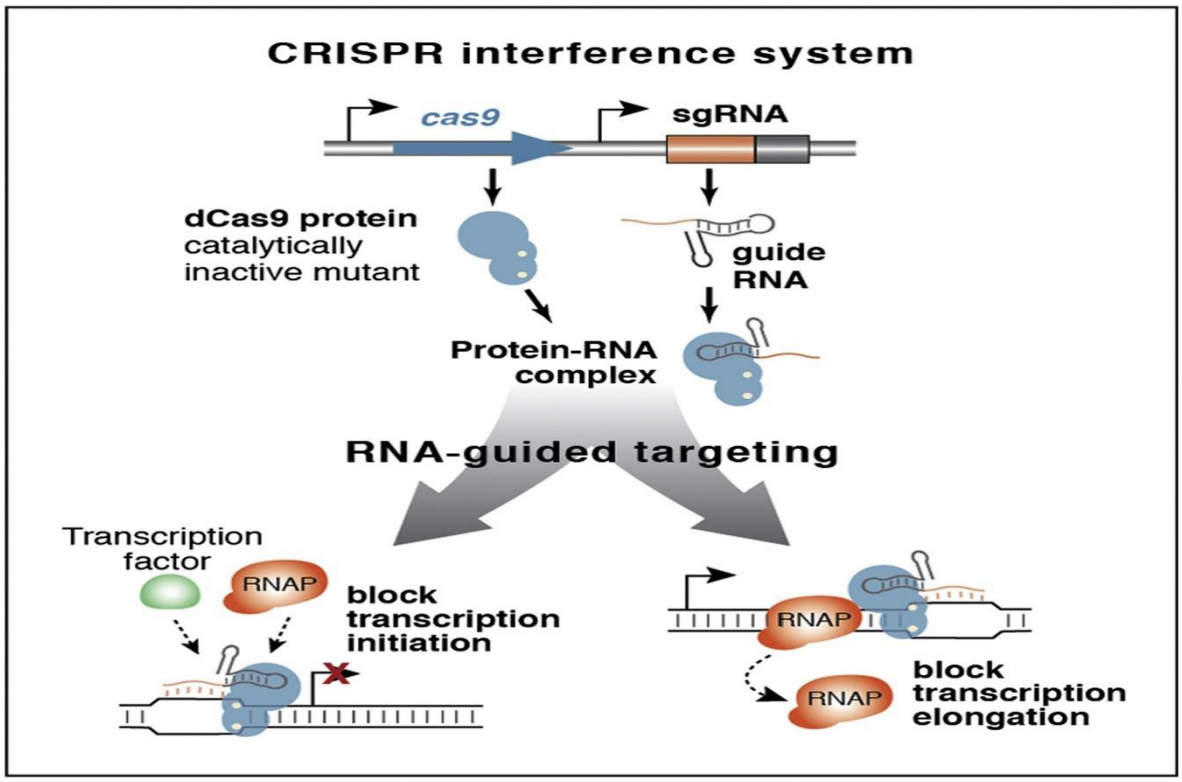

Figure 2.1: Schematic representation of CRISPRi approach for gene silencing. RNAP: RNA polymerase, sgRNA: single guide RNA, Cas9: CRISPR-associated protein 9 (Qi *et al*, 2013).

To achieve the *Rv3218* knockdown in *Mtb* H37Rv, the *Rv3218* specific complementary sequence was cloned into the sgRNA expression cassette in the PLJR965 plasmid. This included firstly the manual design of the single guide-RNA that targets the *Rv3218* gene sequence. The sgRNA was designed to target the non-template strand within the ORF of *Rv3218* which allows for the most efficient gene silencing, and the targeting required the Watson-Crick base pairing and the use of suitable strong PAM sequence which was identified from the list of PAM sequences in table 1.2. This was then followed by the digestion of a large plasmid (PLJR965) with a restriction enzyme (BsmBI) to clone the sgRNA. The transcriptional repression was mediated by the exploitation of the Anhydrotetracycline (ATc) which was directed to the specific DNA target by ATc-inducible sgRNA which inhibits transcription initiation or elongation.

Table 1.3. The list of published PAM sequences together with their fold repression ability and their standard deviation

PAM	Fold repression	SD
5'-NNAGAAG-3'	216.7	10.0
5'-NNAGAAT-3'	216.2	10.4
5'-NNAGAAA-3'	158.1	22.8
5'-NNGGAAG-3'	145.2	5.3
5'-NNAGAAC-3'	120.5	7.9
5'-NNGGAAA-3'	110.5	26.4
5'-NNAGCAT-3'	84.6	5.2
5'-NNAGGAG-3'	82.2	9.2
5'-NNAGGAT-3'	64.7	8.7
5'-NNAGCAA-3'	53.4	9.9
5'-NNGGAAC-3'	51.5	6.2
5'-NNGGAAT-3'	47.3	3.3
5'-NNAGCAG-3'	42.2	7.0
5'-NNAGGAA-3'	38.5	5.2
5'-NNAGGAC-3'	25.5	0.8
5'-NNGGGAG-3'	24.7	1.9
5'-NNGGGAT-3'	24.2	3.4
5'-NNGGGAA-3'	12.3	0.8
5'-NNAGCAC-3'	11.9	1.2
5'-NNGGGAC-3'	7.9	1.0
5'-NNGGCAT-3'	6.7	0.9
5'-NNGGCAG-3'	4.0	0.3
5'-NNGGCAA-3'	3.3	0.3
5'-NNGGCAC-3'	2.7	0.3
ctrl sgRNA	1.3	0.1

2.7.1 Primer design

To clone the *Rv3218* sg-RNA, two oligonucleotides were designed; forward primer which corresponded to the sgRNA sequence, and the reverse primer which was the reverse complement of the forward primer. Firstly, the PAM sequence for designing the sg-RNA was identified downstream of the target sequence on the non-template strand. The sg-RNA sequence was designed to be 20 nucleotides long. Since transcription in mycobacterial species initiates most efficiently with the nucleotide A or G, the sequences were designed in a way that the 20th nucleotide is A or G. The primers were designed to have the dcas9 handle sequences for binding with the dcas9 from the CRISPRi backbone vector PLJR965. The BamHI sequence was included in the primers for plasmid DNA confirmation or screening. Primers used in this study were ordered from Inqaba Biotechnologies, South Africa.

Table 1.4. Primer sequences used in this study

Genes	Primer sequence (5' – 3')	Description
Rv3218	Forward: **ggga**ggatccgcggctttcgagggcgtgcg Reverse: **aaac**cgcacgccctcgaaagccgc**ggatcc**	21' bp of the *Rv3218* sequence yielding an sgRNA that binds to the dCas9 of PLJR965
Knockdown screening	Forward: gcggctttcgagggcgtgcg Reverse: ggagaaaggcggacaggtat	Screening primers that yield a 507 bp amplicon. Forward primer binds at 155 to 174 bp of *Rv3218* sequence and reverse primer binds at 561 to 681 bp of PLJR965

Bold: dCas9 handle sequences, **Bold**: BamHI sequence

2.7.2 Annealing of the oligonucleotides

The annealing process involves two single stranded oligonucleotides that have complementary sequences with heating followed by cooling. Heating is said to break all the hydrogen bonds leading to the disruption of any secondary structure within each oligonucleotide and cooling facilitates hybridization as new hydrogen bonds form between the complementary sequences. The oligonucleotides that were used in this study were annealed using a thermocycler (Bio-Rad T100 Thermal Cycler, Lasec). Briefly, a volume of 4 µL of each oligo (forward and reverse strand; stock concentrations 100 µM in water) was added to 42 µL of annealing buffer (10mM Tris, pH7.5; 50mM NaCl; 1Mm EDTA) to a total of 50 µL. The reaction was performed in 0.5 mL PCR tubes. The primers were annealed in a thermal cycler (Bio-Rad T100 Thermal Cycler, Lasec) with the following program: heating at 95 °C for 2 min followed by cooling at 25°C for 15 min.

2.7.3 Ligations of the CRISPRi backbone (PLJR965) DNA and the annealing oligos

The ligation reactions were carried out using Fermentas T4 DNA ligase (5 U/µL) (Thermo Fisher Scientific). For optimal ligation conditions, the molar ratios of 1:1 and 1:2 vector: insert were used in all reactions. A constant amount of 9 ng of BsmBI-digested and heat killed CRISPRi backbone was used for all ligation reactions.

Ligation reactions were set up in 20 µL volumes containing 9 ng digested PLJR965, 1 µL and 2 µL annealed oligos (for 1:1 and 1:2 reactions respectively), 2 µL ligase buffer (Thermo Fisher Scientific), 1 µL T4 DNA ligase and was filled up to 20 µL with sterile distilled water. The reactions were then incubated at room temperature for 2 hours.

2.7.4 Preparation of chemically ultra-competent cells

The XL-10 Gold ultra-competent cells were used because of their highest transformation efficiency and they exhibit faster growth and they generate larger colonies. The XL-10 Ultracompetent cells (5 x 100 µL) were ordered from Agilent Technologies, USA. For making a stock, 5 µL was taken from a 100 µL vial and plated on nutrient agar plate containing 100 µg/mL ampicillin. The plate was then incubated at 37 °C overnight (CO_2 incubator, Thermo Scientific). The Carbon dioxide incubator was used to maintain an optimal environment for cell growth by providing carbon dioxide control in a humidified atmosphere with constant temperatures. The colony was then picked from the plate and re-suspended aseptically on 10 mL of nutrient broth containing 50µg/mL chloramphenicol which was then incubated by shaking at 37 °C overnight. Stocks were made by aliquoting 800 µL of the culture into 200 µL sterile glycerol (Thermo Scientific) on 1 mL micro centrifuge tubes (Eppendorf) and stored at -80°C.

For competent cells, a vile of the frozen stock was added to 10 mL of nutrient broth containing 50µg/mL chloramphenicol on a conical flask and was then incubated by shaking overnight at 37 °C. This step was done to allow treatment of the cells with antibiotics to control contamination. A volume 1 mL of the overnight culture was then added into 50 mL nutrient broth and was then incubated by shaking at 37 °C for 2 hours to ensure that the cells have reached exponential phase. The culture was immediately transferred to 50 mL falcon tubes (Thermo Scientific) and was placed on ice for 10 min followed by centrifuging at 4000 x g for

10 min at 4 °C. The supernatant was discarded and the pellet was re-suspended gently in 1 mL ice cold 100 mM calcium chloride ($CaCl_2$) then transferred into a fresh micro centrifuge (Eppendorf) tube. The cells were centrifuged at 15 000 xg on a table top centrifuge (Centrifuge 5415 D, Eppendorf) for 30 seconds. The supernatant was discarded and the pellet was re-suspended gently in ice cold 100 mM $CaCl_2$. The cells were then incubated on ice for 2 hours.

2.7.5 Transformation of XL-10 ultracompetent cells

This method was followed according to standard procedures for XL10-Gold ultracompetent cells transformation (Agilent, USA). Briefly, two 14-mL BD Falcon polypropylene round-bottom tubes (Thermo Scientific) were pre-chilled on ice (one tube was for the experimental transformation and one tube was for the Puc18 control). The NZY+ broth (detailed on the appendix section) was pre-heated on 42 °C on a water bath (Labotec) for 15 min. The ultra-competent cells were thawed on ice. A volume of 100 µL of cells was gently mixed and aliquoted into each of the pre-chilled 14-mL BD Falcon polypropylene round-bottom tubes. A volume of 4 µL of the ß-Mercaptoethanol (Agilent Technologies) mix was then added to each aliquot of cells. The tubes were swirled gently followed by incubation on ice for 10 min, with swirling every 2 min. A volume of 2 µL of the ligation mixture were added to the tubes for the experimental transformation. The Puc18 control DNA was diluted 1:10 with sdH20, then 1 µL of the diluted Puc18 DNA was added to the other aliquot of cells. The tubes were swirled gently, then incubated on ice for 30 min. the tubes were then heat-pulsed in a 42 °C water bath for 30 seconds. The tubes were incubated on ice for 2 min. 0.9 mL of pre-heated (42°C) NZY+ broth was added followed by incubation at 37 °C for 1 hour with shaking at 225 × g . A volume of 200 µL of the transformation mixture was plated on nutrient agar plates containing the appropriate antibiotic (kanamycin). For the Puc18 control transformation, 5 µL of the transformation was plated on kanamycin plates. All the plates were incubated at 37 °C overnight.

2.7.6 Confirmation of colonies containing the CRISPRi Knockdown

For the confirmation of the colonies containing the knockdown plasmid, bulk plasmid extraction (GeneJet midiprep kit as previously describe in this study) was performed from each colony. After extraction, the DNA was then quantified using a NanoDrop. The extracted plasmid was then digested with BamHI for the analysis of the presence and the orientation of

the insert and for the plasmid size. The restriction digest protocol was as follows: BamHI (10 U/µL), 10X red buffer, and 50 ng of knockdown plasmid DNA. The extracted and restricted plasmids were then separated using gel electrophoresis with the expected band size of 8636 base pairs for the extracted plasmid and double bands for the restricted plasmid; 6067 bp and 2569 bp.

2.8 Electroporation into *Mtb*

Mycobacterium Tuberculosis (Mtb) was grown at 37 °C for 7 days to an OD_{600}nm of 0.6 - 0.8 in a final volume of 100 mL 7H9 media, using a stationary phase pre-culture as an inoculum. The cells were harvested at 2 630 × g for 10 min at 4 °C and the pellet was then washed 4 times by gentle resuspension in consecutive steps of 45 mL, 20 mL, 10 mL and 5 mL of ice-cold 10 % glycerol, followed by centrifugation at 2 630 × g for 10 min at 4 °C. The final cell pellet was re-suspended in 2 mL ice-cold 10 % glycerol and these competent cells were used immediately. Up to 5 µg plasmid DNA was added to a 400 µL aliquot of *Mtb* competent cells. This was transferred to a 0.2 cm electroporation cuvette (Bio-Rad laboratories) and pulsed using the following conditions: 2.5 kV, 25 µF and 1000 Ω in the Electro Cell Manipulator (BTX ECM 630). The cells were rescued immediately with 800 µL 2 × TY for at least 3 hours at 37 °C and thereafter plated on Middlebrook 7H11 media containing the appropriate supplements and antibiotics, followed by incubation for 5 weeks at 37 °C before scoring Colony forming units (CFU).

2.9 DNA manipulation

2.9.1 Cetyltrimethylammonium bromide (CTAB) DNA extraction

Bacterial strains were grown on 7H11 agar for 5 weeks and the resulting cells were harvested by pool scraping the surface of the agar plate and resuspending the cells in 500 µL TE buffer followed by incubation at 65 °C for 35 min. The cells were incubated at room temperature to cool down. Thereafter, a 50 µL aliquot of lysozyme (10 mg/ml) was added to the sample and incubated at 37 °C for 1 hour, subsequently 70 µL of 10 % SDS and 6 µL of proteinase K (10 mg/mL) was added and the sample was incubated at 65 °C for 2 hours. Following incubation,

100 µL 5 M NaCl and 80 µL pre-warmed CTAB/NaCl was added, mixed and incubated at 65 °C for 10 min. An equal volume of 24:1/Chloroform:Isoamyl alcohol was added, followed by mixing and centrifugation at maximum speed for 5 min at room temperature. The aqueous layer was subsequently transferred into a fresh Eppendorf tube followed by the addition of 0.6 volume equivalent isopropanol and centrifugation for 20 minutes at room temperature. The supernatant was discarded, and the pellet was washed in 70 % ethanol followed by drying using an Eppendorf Concentrator 5413 D. The DNA pellet was resuspended in 50 µL sterile distilled water (sdH2O) and quantified using NanoDrop and stored at 4 °C.

2.9.2 Screening of positive knockdown mutants

The extracted DNA was then used in PCR reactions using DreamTaq (Thermus aquaticus) Polymerase for the screening of positive knockdown mutants. Taq polymerase was chosen because of its ability to amplify fragments at much higher temperatures without denaturing. PCR reactions were set up in 25 µL volumes containing 1X DreamTaq polymerase buffer, 0.2 mM dNTP, 0.5 µM forward and reverse primers (*Rv3218* gene specific forward and CRISPRi universal reverse), 50 ŋg template DNA and 1.25 U DreamTaq DNA polymerase. The reactions were then incubated in a thermo cycler with the following parameters: the initial denaturation at 95 °C for 3 minutes, followed by denaturation at 95 °C for 30 seconds for about 35 cycles, annealing temperature which was dependable on each set of primers used for 30 seconds, then first extension at 72 °C for 1 minute, which was then followed by the final extension at 72 °C for 10 minutes.

2.10 Analysis of bacterial growth

2.10.1 Growth patterns analysis

For the analysis of the growth patterns of wild type and knockdown strain, growth curve experiments were conducted. For this, a pre-culture was set up by inoculating 1 mL of frozen culture into 10 mL 7H9 containing 25 µg/mL Kanamycin for the mutant strain. The cultures were then incubated overnight at 37 ºC shaking at 100 rpm. The preculture was then diluted to a final OD600nm of 0.05 in 50 ml 7H9 media. The cultures were made in triplicates; Wild type, *Rv3218* mutant without ATc and *Rv3218* mutant with 100 ng/mL ATc. The cultures were then

incubated at 37ºC for 16 days. Growth was determined by recording OD600nm measurements at 24 hour intervals and data was displayed as a line chart.

2.11 Minimum Inhibitory Concentrations (MICs)

The Minimum Inhibitory Concentrations (MIC) for each agent against the *Mtb* H37Rv wild type and the *Rv3218* knockdown were determined by means of broth microdilution method using the Middlebrook 7H9 broth (Difco, United States). Each antibiotic was preliminary dissolved to obtain a stock solution which was then diluted to get an appropriate starting concentration. The solvents that were used in this study were water and alcohol, depending on the type of antibiotics. All the required antibiotics that were used in this study were from Sigma-Aldrich (St. Louis, USA) and they are: Ofloxacin, Meropenem, Erythromycin and Colistin sulphate salt. Stock for Ofloxacin (1mg/mL) was prepared using sterile distilled water, Meropenem (100mM) was also dissolved with sterile distilled water, Erythromycin (10mg/mL) was dissolved in 95 %ethanol and Colistin sulphate salt (50mg/mL) was dissolved in sterile distilled water. The working concentrations were as follows: Ofloxacin (25.6 – 0.02) µg/mL, Meropenem (128 – 0.02) µg/mL, Colistin Sulphate salt (32 – 0.03) µg/mL, Erythromycin (160 – 0.12) µg/mL.

Bacterial strains were grown until an OD_{600}nm of 0.3 was reached. Microtiter plates were set up using 96 well plates containing 12 rows (row 1 to row 12) with rows 11 and 12 containing the positive and the negative controls respectively. The positive control was the bacterial cultures without antibiotics, and the negative control was sterile 7H9 broth. Antibiotic stocks containing the initial concentrations for each antibiotic (Ofloxacin 25.6 µL/mL, Meropenem 128 µL/mL, Colistin Sulphate Salt 32 µL/mL, Erythromycin µL/mL) were set up on 1 mL tubes (Eppendorff). Thereafter, a 100 µL volume of the antibiotic stocks was inoculated into first row of the microtiter plate for each antibiotic. Following that, a volume of 50 µL of 7H9 media was inoculated into row 2 to row 10. An aliquote of 50 µL of the antibiotic stock from row 1 from each antibiotic was inoculated into row 2 followed by mixing, and 50 µL was aliquoted from row 2 into row 3. This was done through to row 10 and 50 µL was aliquoted from row 10 and discarded since row 11 and 12 were controls. The bacterial cultures (OD_{600}nm 0.3) were diluted 1000 folds on 14 mL tubes and 50 µL of the diluted cultures was added to

each well (excluding row 12). The plates were sealed on plastic bags and incubated in an atmosphere of 5 % CO_2 with a relative humidity of 37 °C for 7 days. Plates were checked after 24 and 72 hours for contamination. The plastic bags were critical to prevent evaporation of the culture in the wells and was also essential for biological containment. This was also done to prevent the risk of accidental spillage during handling. The plates were read inside the biological cabinet. For all the antibiotics, the lowest antimicrobial concentration with no visible growth was considered to be the MIC.

2.12 Osmolarity Assay

Osmolarity is a dynamic and fundamental physiochemical property of microbial environments. Different microbial species use different characteristics, including their cell wall components and cell wall genes for survival in different osmolarity conditions. In *Mtb*, the *Rv3218* mutant (hypothesized to be a dgk), is said to not grow competently on nutrient media of low osmolarity (Raetz and Newman, 1977). In this study, to assess whether the *Rv3218* mutant strains grow on nutrient media of low osmolarity, growth of the wild-type strain was compared to the growth of the knockdown strain on a liquid media with altered osmolarity. Sauton's media was the media of choice and Sodium Chloride (NaCl) was the base that was used to adjust the osmolarity.

Sauton's Minimal Media with different NaCl concentrations (0 %, 0.5 %, 2 %, 5 % and 10 %) were prepared. Firstly, 1 mL frozen stocks of each strain; wild type and mutants, was grown onto 10 mL 7H9 broth on 50 mL cell culture flasks (Lasec) until OD_{600}nm of 1.6 was reached. Following this, the wash step was required for the total removal of the 7H9 since a different media (Sauton's media) was going to be used. This was conducted by transferring the bacterial culture into 50 mL falcon tubes (Lasec) and centrifuging (Multifuge 3 S-R, Thermo Scientific, Germany) for 20 minutes at 4000 *xg*. The supernatant was then discarded and the pellet was resuspended in 10 mL Sauton's Minimal Media (without NaCl). The wash process was repeated 2 times to be certain that the 7H9 media was completely washed off. The pellet from the second wash was then resuspended in 10 mL Sauton's Minimal Media in order to obtain the inoculum. From the inoculum, the OD reading was taken to check if the OD readings taken before washing did not change. Following that, for each NaCl concentration, three 20 mL minimal media cultures were set up on 200 mL cell culture flasks with ventilation caps (Lasec), these included (i) Wild type, (ii) Knockdown with no ATc, (iii) Knockdown with ATc (100

ng/mL). The cultures were set up with a starting OD_{600}nm of 0.05 and incubated at 37 °C in a CO_2 incubator (Thermo Scientific). Growth patterns of wild type and knockdown strains were determined by conducting growth curve experiments. Optical Density readings were taken 24 hours apart for 15 days until death phase.

2.13. Statistical analysis

All data for all the triplicate cultures from the conducted experiments were recorded into Microsoft Excel sheet and were then analysed using a statistical analysis t-test. The data was tabulated using OD 600 nm readings, mean (AV), and standard deviation (SD). The mean was necessary for finding the p-value which determines the statistical significance between the samples, and the standard deviation was necessary for determining the error bars for each experiment. A p-value <0.05 was used as a reference to institute statistical significance of comparisons.

Chapter 3: Results

3.1 Bioinformatics analyses of the *Rv3218* gene

In this study, we allowed use of some bioinformatics softwares and tools to predict the function of a hypothetical protein, *Rv3218* identified from the *Mtb* H37Rv genome (strain ATCC25618). As the initial means of identifying the function of the *Rv3218* gene, we first searched it on Mycobrowser (Mycobacterial browser), which is a comprehensive and extensive genomic and proteomic data receptacle for infectious mycobacteria. It provides manually-curated gene annotations and suitable tools to advance proteomic and genomic research of these organisms. On mycobrower, the *Rv3218* gene was found to be 966 bp long, located at 3594468 bps on the positive strand of the *Mtb* genome and is situated 519 bp downstream of *Rv3217c* (**Figure 3.1.1**) the protein product of which is a probable conserved integral membrane protein, and 700 bp upstream whiB1 gene which is a regulatory protein involved in transcriptional mechanism. The *Rv3218* gene was found to have a molecular mass of 34474.5 Da, isoelectric point of

9.2926 and a protein length of 321 amino acids. Also found to be similar to several hypothetical bacterial proteins which include the Q9F3M0|2SC7G11.03c from *Streptomyces coelicolor* (322 aa), Q9A0J4|SPY0752 from *Streptomyces pyogenes* (340 aa) and O31502|YERQ from *Bacillus subtilis* (303 aa); where aa stands for amino acids. Overall, from the findings above, the *Rv3218* gene is predicted to code for a probable cell wall protein and functions in cell wall processes, and is also thought to be a transcription regulator.

One other important aspect to look at when searching for a function of a hypothetical protein is to look at its orthologues. Orthologues are defined as proteins or genes in dissimilar species that are thought to have evolved from the same or a common ancestral gene by speciation, and as a result, orthologues keep the same function or activity during the course of evolution (Fang *et al.*, 2010). By looking at and knowing the function of the orthologues of the gene, one can be able to predict the function of a given gene. The identification of orthologues is an evaluative process for reliable forecast of gene function in recently sequenced genomes. The *Rv3218* gene orthologues include Mb3244 from *M. bovis*, ML0805c from *M. leprae*, MMAR_1339 from *M. marinum*, MSMEG_1920 from *M. smegmatis*. These orthologues are conserved proteins that are predicted to have kinase activities. **Figure 3.1.1** shows the location of the *Rv3218* gene on the *Mtb* genome, and the neighbouring genes as seen on Mycobrowser.

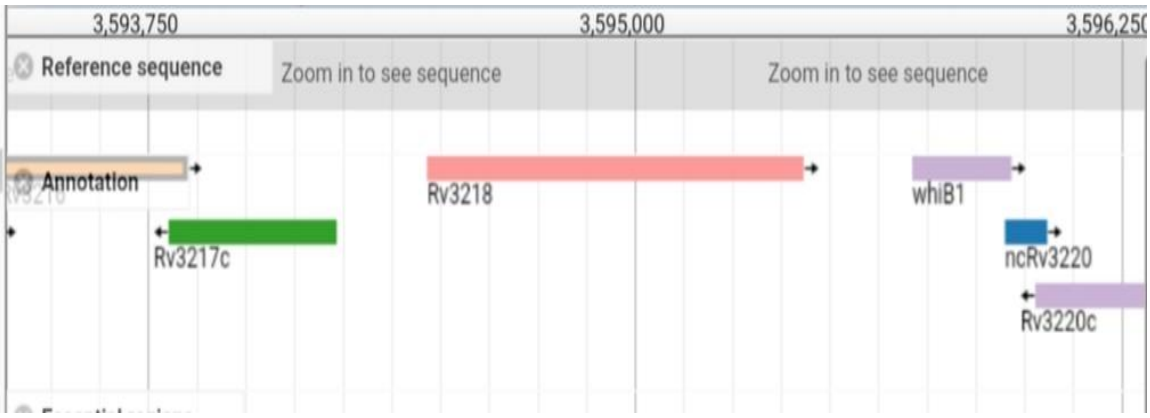

Figure 3.1.1: illustration of the localisation of the *Rv3218* gene and the neighbouring genes on the *Mtb* genome on the Mycobrowser online tool.

Searching for functional domains and crucial regions of the protein is another important stride on Hypothetical protein function prediction and characterization. Domains are structural and

functional parts of a protein, which are normally associated to particular function or interaction, partaking to the functionality of the protein at large (Basu *et al.*, 2009; Silva *et al.*, 2020). In this regard, pfam was used. Pfam is one of the most useful databases of protein families and their domains that is extensively used to study novel genomes, metagenomes and to conduct experimental activity on certain proteins and systems (Mistry *et al.*, 2021). When the protein sequence of *Rv3218* was searched on pfam, it was found to have a predicated molecular function of a kinase activity where it is predicted to be involved in the catalysis of the transfer of a phosphate group, usually from ATP, to a substrate molecule. The similar proteins were the DAGKc domain-containing proteins from different species which include *Colletotrichum fioriniae* and many more. Searching for *Rv3218* conserved domains on InterProScan was feasible to identify important components that corroborate with Mycobrowser results, conveying that *Rv3218* has domains that are mainly conserved in different families of kinases, mainly the diacylglycerol kinase.

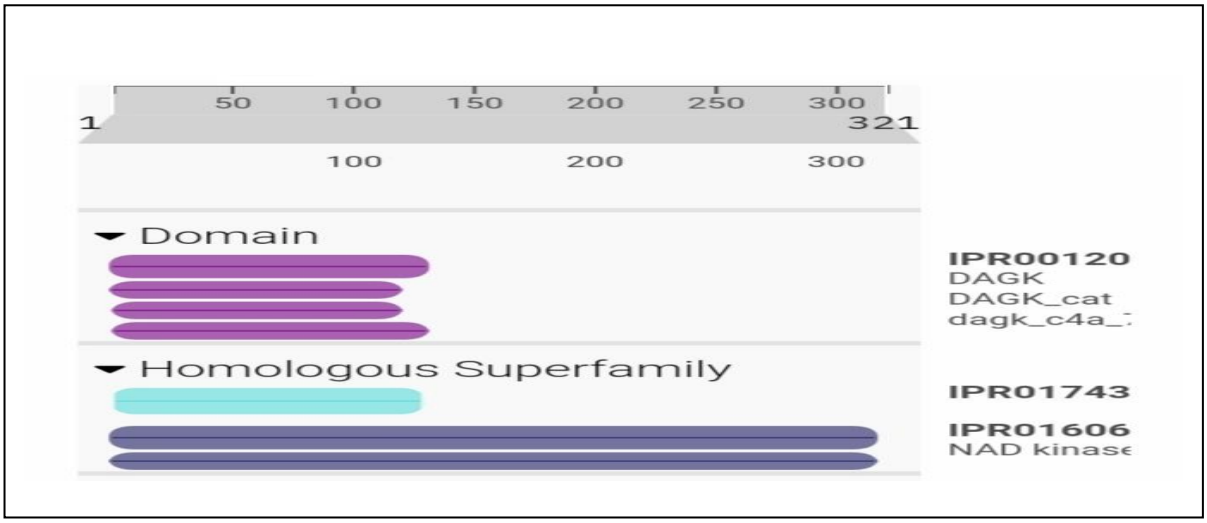

Figure 3.1.2: Results for functional domains, families and essential regions of the *Rv3218* hypothetical protein. Results obtained by InterProScan platform. Purple lines represent the closely related domains, blue line represents the homologous superfamily, and the strong blue lines represent the neighbouring superfamilies.

Specifically, **figure 3.1.2** (extracted from InterProScan) shows domains and the homologous superfamilies' of *Rv3218* gene. A homologous superfamily is a family or a group of proteins that have the same evolutionary origin, shown by their structural similarities (Bray *et al*, 2000).

The *Rv3218* protein shares similar catalytic domain with the number of Diacylglycerol kinases that serve as protein kinase C activators with their catalytic domain presumed from the discovery of bacterial homologues including the *Escherichia coli YegS* protein. *Rv3218* gene also shows regions of resemblances with some proteins of a homologous superfamily, Diacylglycerol kinase, including the Nicotinamide Adenine Dinucleotide (NAD) kinase which also function in cell wall processes. This shows that not only that the protein may be related to kinase metabolism, but it indicates that R*v3218* probably shares evolutionary origins with the other proteins in this homologous superfamily. On InterProScan it was also shown that the closely related structure of *Rv3218* protein (**Figure 3.1.3**) was the diacylglycerol kinase structure that represented 100% similarities. **Figure 3.1.4** shows the *Rv3218* most similar structural models from other microorganisms as seen on iTASER. The most closely related (model **A** and **B**) are both *YegS* genes from *E. coli* and *Salmonella typhimurium* which are also annotated as probable lipid kinases.

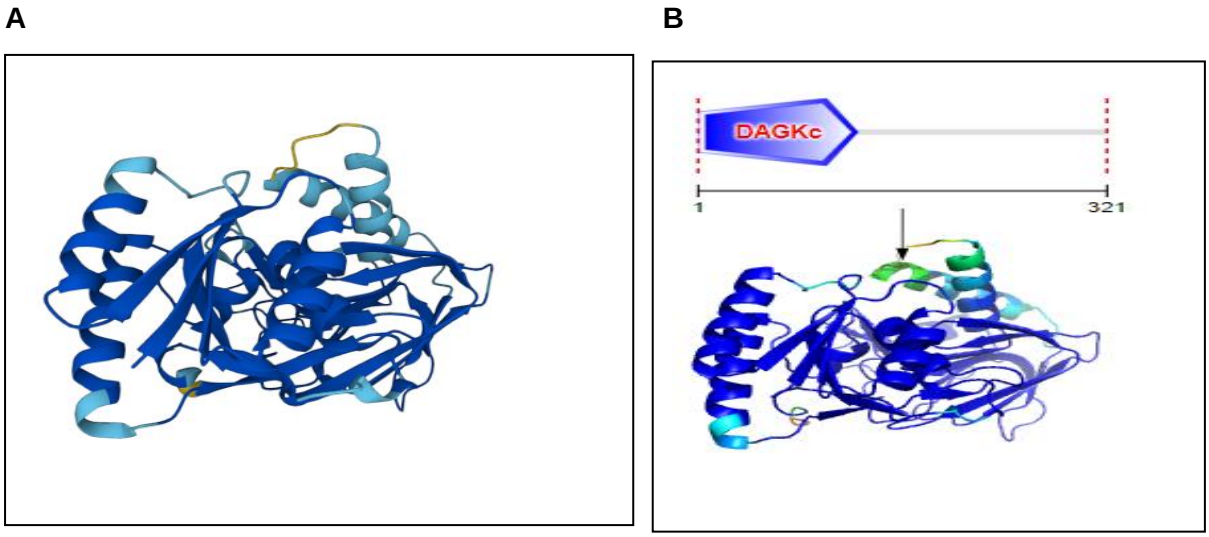

Figure 3.1.3. Predicted 3D structural depiction of the hypothetical protein *Rv3218* performed by comparison with the 3D structure of Diacylglycerol kinase. The *Rv3218* protein structure **(A)** represents 100% similarity with the Diacylglycerol kinase structure **(B).**

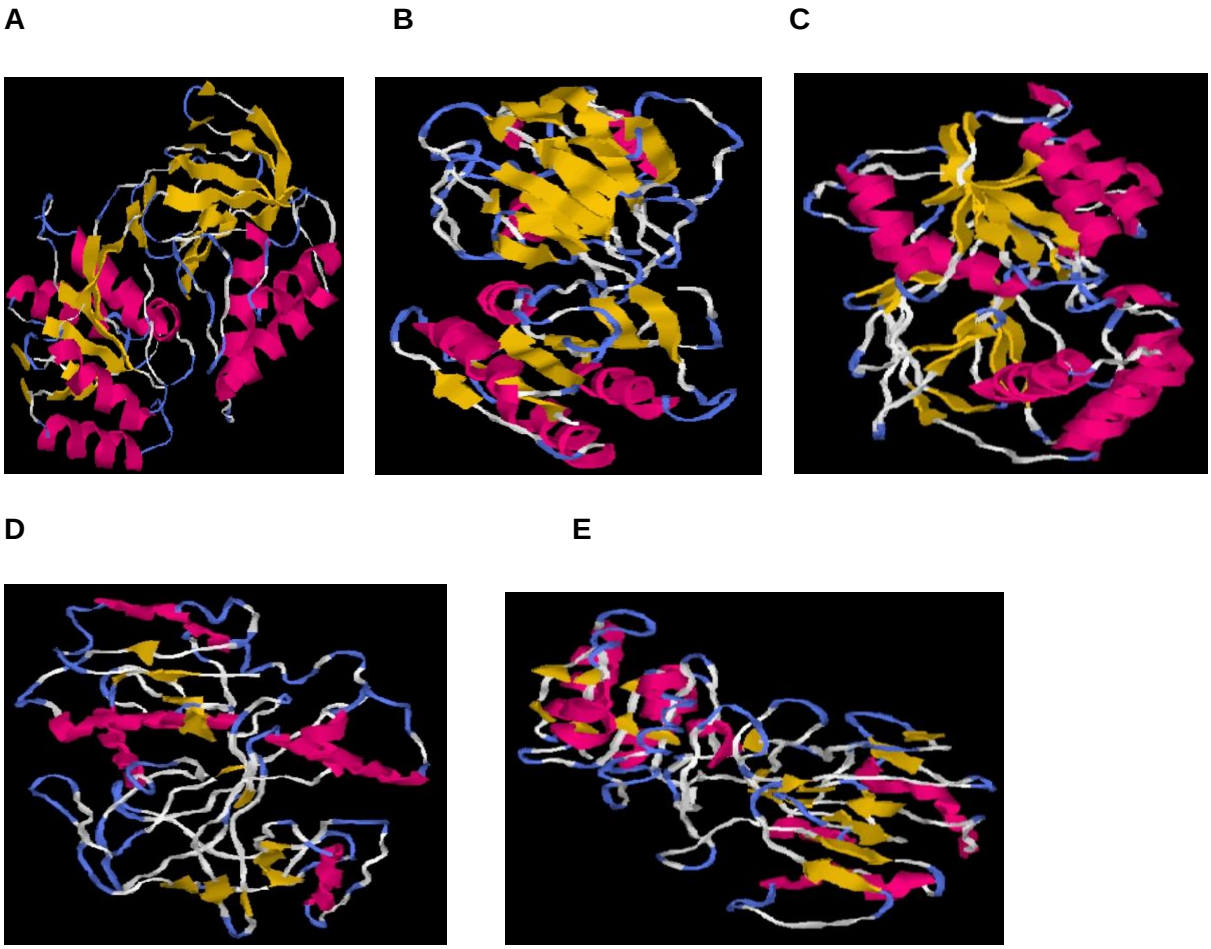

Figure 3.1.4: Illustration of *Rv3218* closely related structural models from iTASER. Relation decreases from **A** to **E**. The most closely related (model **A** and **B**) are both *YegS* genes from *E. coli* and *Salmonella typhimurium* which are also annotated as probable lipid kinases.

Another way of predicting the protein function is to look at its interactions. Proteins and their functional interactions institute the foundation of the cellular machinery and the way they are connected needs to be considered for the comprehensive knowledge of biological phenomena (Szklarczyk, 2019). The STRING (v11.5) database focuses on collecting, scoring and integrating all publicly obtainable origins of protein–protein interaction details, and to supplement these with computational forecasts. Its main objective is to attain a comprehensive and objective global network, including both physical and functional interactions (Szklarczyk, 2019). **Figure 3.1.5** below (STRING v11.5) shows *Rv3218* protein interaction with other

proteins. Coloured circle nodes represent proteins that are first shell of interactors, and the lines represent protein-protein associations, meaning that the *Rv3218* proteins jointly contributes to a shared function with each protein that appears on the list and this does not automatically mean that they are physically binding to each other. The known interactions are represented in blue lines.

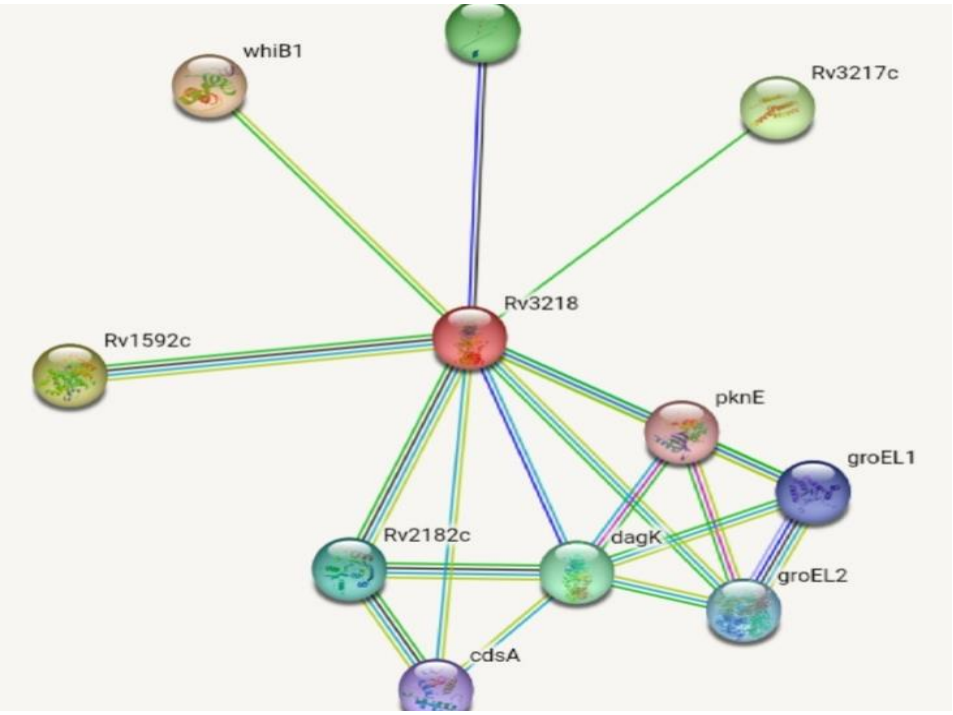

Figure 3.1.5: Illustration of *Rv3218* gene and its interacting protein. Image extracted from STRING database.

On STRING, we also looked at gene co-occurrences. Co-occurrence of proteins and genes in sequenced genomes depends on the fact that proteins do not work or function in isolation and are reliable on other proteins, either as direct binding partners, or as catalysts of substrates (Muller and Ancuso, 2008). We found that gene co-occurrence in *Mtb*H37rv strain denoted a 100% similarity between the *Rv3218* protein and diacylglycerol kinase.

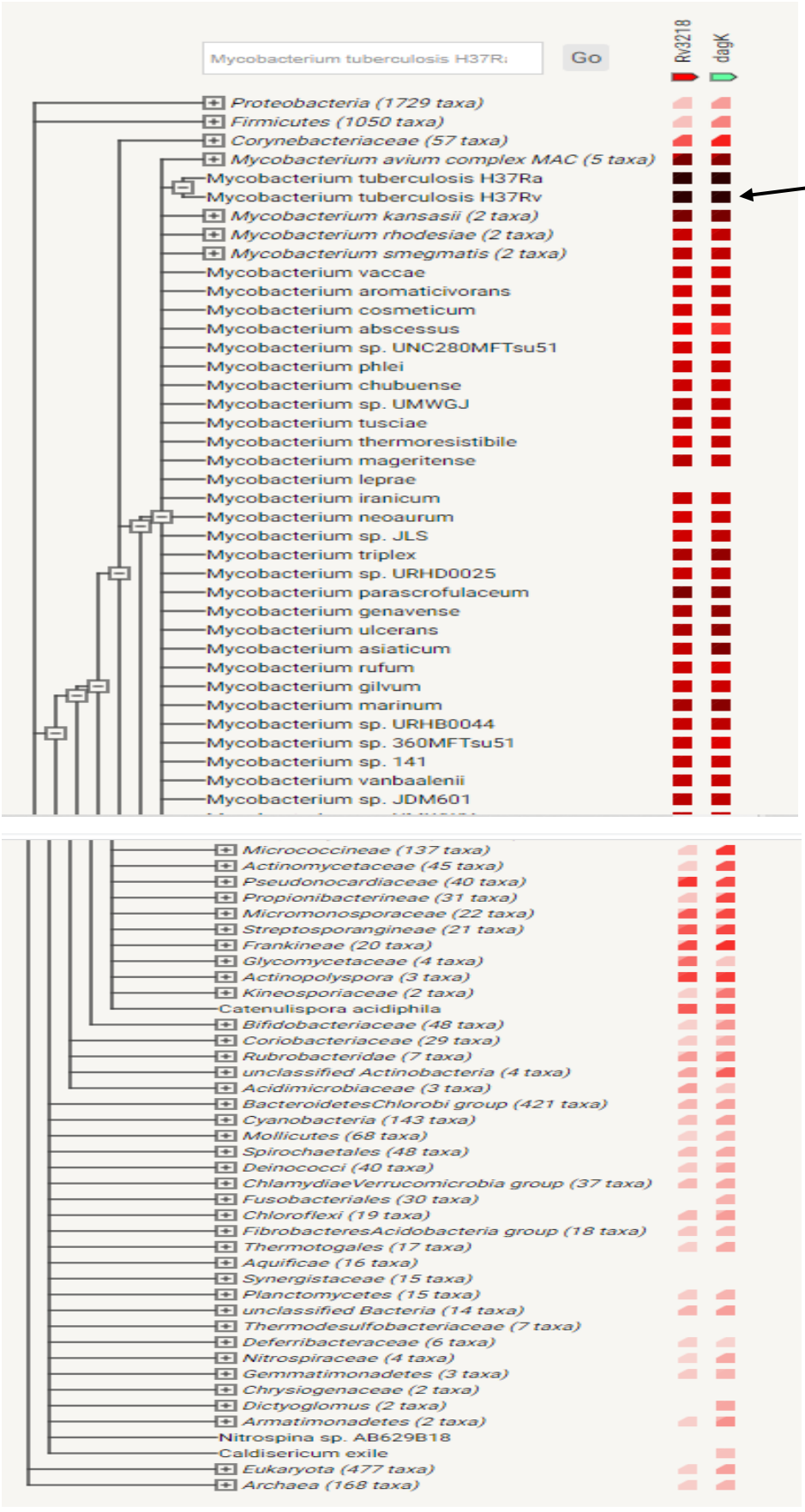
Mycobacterium tuberculosis H37R
Go
Rv3218
dagK
Proteobacteria (1729 taxa)
Firmicutes (1050 taxa)
Corynebacteriaceae (57 taxa)
Mycobacterium avium complex MAC (5 taxa)
Mycobacterium tuberculosis H37Ra
Mycobacterium tuberculosis H37Rv
Mycobacterium kansasii (2 taxa)
Mycobacterium rhodesiae (2 taxa)
Mycobacterium smegmatis (2 taxa)
Mycobacterium vaccae
Mycobacterium aromaticivorans
Mycobacterium cosmeticum
Mycobacterium abscessus
Mycobacterium sp. UNC280MFTsu51
Mycobacterium phlei
Mycobacterium chubuense
Mycobacterium sp. UMWGJ
Mycobacterium tusciae
Mycobacterium thermoresistibile
Mycobacterium mageritense
Mycobacterium leprae
Mycobacterium iranicum
Mycobacterium neoaurum
Mycobacterium sp. JLS
Mycobacterium triplex
Mycobacterium sp. URHD0025
Mycobacterium parascrofulaceum
Mycobacterium genavense
Mycobacterium ulcerans
Mycobacterium asiaticum
Mycobacterium rufum
Mycobacterium gilvum
Mycobacterium marinum
Mycobacterium sp. URHB0044
Mycobacterium sp. 360MFTsu51
Mycobacterium sp. 141
Mycobacterium vanbaalenii
Mycobacterium sp. JDM601
Micrococcineae (137 taxa)
Actinomycetaceae (45 taxa)
Pseudonocardiaceae (40 taxa)
Propionibacterineae (31 taxa)
Micromonosporaceae (22 taxa)
Streptosporangineae (21 taxa)
Frankineae (20 taxa)
Glycomycetaceae (4 taxa)
Actinopolyspora (3 taxa)
Kineosporiaceae (2 taxa)
Catenulispora acidiphila
Bifidobacteriaceae (48 taxa)
Coriobacteriaceae (29 taxa)
Rubrobacteridae (7 taxa)
unclassified Actinobacteria (4 taxa)
Acidimicrobiaceae (3 taxa)
BacteroidetesChlorobi group (421 taxa)
Cyanobacteria (143 taxa)
Mollicutes (68 taxa)
Spirochaetales (48 taxa)
Deinococci (40 taxa)
ChlamydiaeVerrucomicrobia group (37 taxa)
Fusobacteriales (30 taxa)
Chloroflexi (19 taxa)
FibrobacteresAcidobacteria group (18 taxa)
Thermotogales (17 taxa)
Aquificae (16 taxa)
Synergistaceae (15 taxa)
Planctomycetes (15 taxa)
unclassified Bacteria (14 taxa)
Thermodesulfobacteriaceae (7 taxa)
Deferribacteraceae (6 taxa)
Nitrospiraceae (4 taxa)
Gemmatimonadetes (3 taxa)
Chrysiogenaceae (2 taxa)
Dictyoglomus (2 taxa)
Armatimonadetes (2 taxa)
Nitrospina sp. AB629B18
Caldisericum exile
Eukaryota (477 taxa)
Archaea (168 taxa)

Figure 3.1.6: Schematic representation of the co-occurrence between *Rv3218* and Diacylglycerol kinase in different bacterial species, including the *Mtb* H37Rv. The black arrow points at *Mtb* H37rv. The darker shades represent 100 % similarity and the lighter shades represent no similarity.

Overall, these results indicate that the *Rv3218* protein is similar to Diacylglycerol kinase. However, laboratory experiments were done in order to confirm this hypothesis.

3.2. Construction of *Rv3218* knockdown

Gene knockdown is a molecular technique which is one of the major strategies that have been used in molecular and cell biology research to establish the function or role of a particular gene. In this study, we followed the method of a CRISPRi system that is based on the ability of dead Cas9 protein in compound with the sgRNA to bind specifically to the target gene and sterically block transcription and elongation at the sgRNA base-pairing genomic locus (Evsyutina *et al.*, 2022).

In the approach that was followed, dCas9 is directed by inducible sgRNA to a target sequence in the genome, from where it binds but does not cleave the DNA. Consequently, the dCas9 can prevent transcription when it binds to the regulatory region or the promoter of the targeted gene which in this case its *Rv3218* gene. The DNA sequence does not get altered, so when the cell naturally clears the dCas9 enzyme, the targeted gene is free to be expressed again.

For a specified gene knockdown, we synthesized, annealed and cloned the target-specific complementary oligonucleotide sequences into BsmBI-digested PLJR965 backbone that carries the dcas9 cassette as described in Materials and Methods section. The BsmBI special restriction enzyme introduces editable overhangs in order to circumvent the addition of more nucleotides in the course of the assembly of the sgRNA. For marking the proper target site for binding, the PAM sequence, situated below the specific forward primer in the *Rv3218*

sequence, was found to be **AGCAG**, which is amongst the list of the PAM sequences that are regarded as 'strongest' from the published PAM consensus for Sth1 dcas9 (Rock, 2017) as illustrated on Materials and Methods section. The sgRNA was designed in a way that it is made up of mainly two regions, the 5′ variable region that is specific for target DNA binding, and the 3′ constant region that binds to the dCas9.

For *in vitro* experiments, we firstly did bulk plasmid extraction of PLJR965 plasmid followed by digestion with BsmBI. The restricted plasmid was then heat killed at 85 °C on a heating block. Heating at higher temperatures result in the complete inactivation of the restriction enzyme so that it does not compete with the ligase enzyme during ligations. The plasmid was then run on an agarose gel electrophoresis (using a 1kb GeneRuler) as described on the Materials and Methods section. **Figure 3.2.1** confirms that the restricted plasmid displayed expected sizes predicted for the PLJR965 plasmid which is 8606 bps for the cut plasmid. **Figure 3.2.1 A** corresponds with the predicted plasmid map and the expected banding patterns. The extracted and restricted plasmid was then ligated with the annealed oligos followed by transformation as described in the Materials and Methods section. After transformation, four colonies were picked after an overnight incubation. Bulk plasmid extraction was performed on the chosen colonies, the plasmid DNA was then digested with BamHI followed by fragmentation on gel electrophoresis as described previously. The sizes were 8636 bps for the unrestricted knockdown plasmid, and for the restricted knockdown it was 6067 bps and 2569 bps.

A

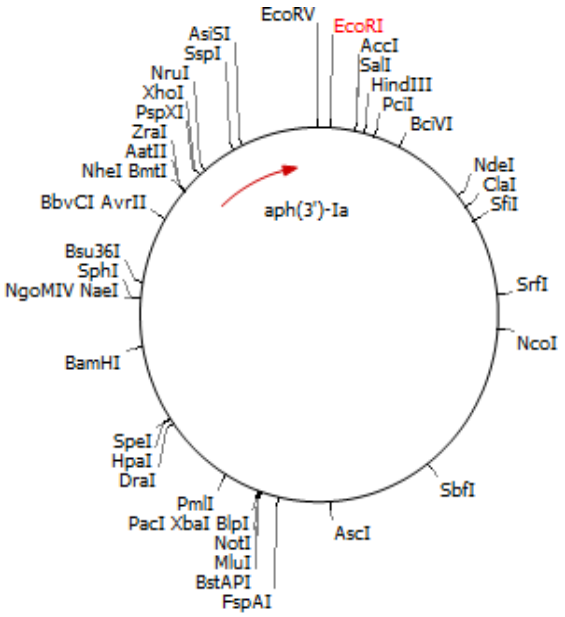

B

Restriction Enzyme	Expected sizes (bp)
BsmBI	8606

C

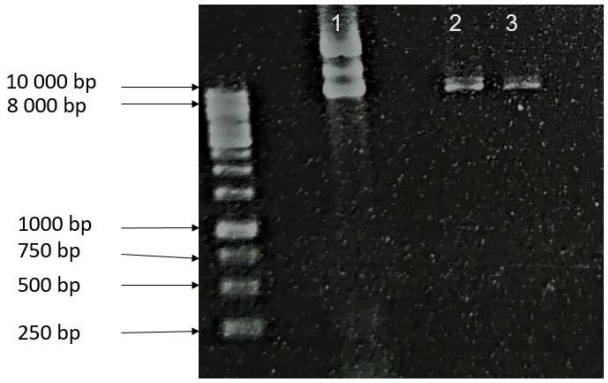

Figure 3.2.1: (**A**) Illustration of the PLJR965 plasmid construct that was used in this study. The plasmid map was generated using SnapGene viewer and the clone manager software. (**B**) Shows the plasmid sizes after restriction. (**C**) Gel image of unrestricted (lane 1) and restricted PLJR965 (lane 2 and 3; 8606 bp)

.

A

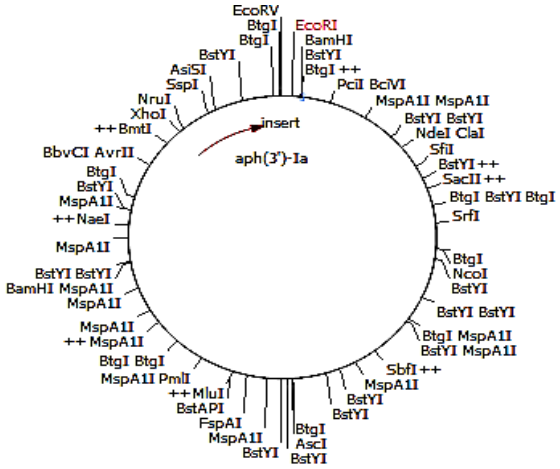

B

Restriction enzymes	Expected sizes (bp)
BamHI	6067
	2569

C

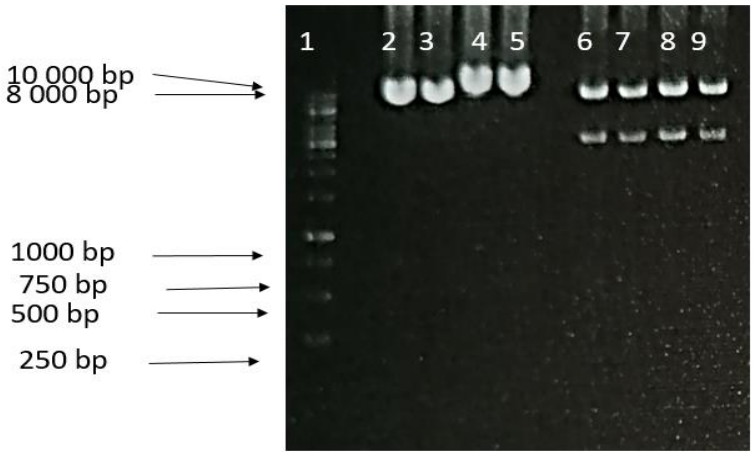

Figure 3.2.2: Illustration of the *Rv3218* gene knockdown plasmid constructed using a CRISPRi dcas9 system. **A** Shows the knockdown plasmid map generated on clone manager. **B** shows the prediction of band sizes for the digested *Rv3218* gene knockdown as shown on clone manager software. **C** shows the gel image (using 1 kb generuler) of unrestricted knockdown (lane 1 - 4) at the band size of 8636 bps and restricted knockdown (lane 6-9) at the band size of 6067 bps and 2569 bps as seen on clone manager.

After confirming the colonies with the *Rv3218* gene knockdown, the knockdown plasmid was introduced to *Mtb* cells via electroporation as described in the materials and methods section. After electroporation, the cells were plated on Middlebrook 7H11 media containing the appropriate antibiotics as described on materials and methods section, followed by incubation for 5 weeks at 37 °C before scoring Colony forming units (CFU).

After scoring the colony forming units, DNA was extracted from the colonies using the CTAB method as described in the Materials and Methods section. We then used the DNA (489.5 ng/uL) for the screening of positive knockdown mutants via a polymerase chain reaction. **Figure 3.2.3** shows a fragment (507 bp) generated by amplifying the CRISPRi universal reverse primers and specific forward primers.

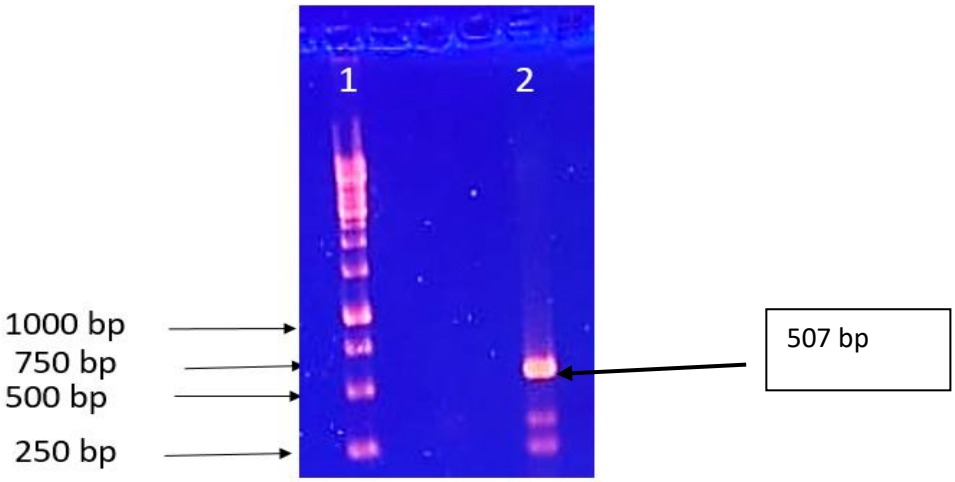

Figure 3.2.3: Gel image results for the screening of positive mutants showing amplification at 507 bps. Lane 2 shows the correct band size (507 bp).

From these results, we can conclude that the CRISPRi dcas9 gene knockdown was successful as all the predicted size for all the steps were obtained. From here, we then further on tested the effect of this gene knockdown on the growth of *Mtb* on 7H9 media and stated on the materials and methods section.

3.3 Growth patterns analysis

Bacterial growth can be more prone to variations due to changes in internal and environmental conditions (Vidal *et al.,* 2022). The analysis of bacterial growth play a principal role in the discovery of the regulation of gene expression and in the development of modern microbial physiology (Klumpp and Hwa, 2014). Here, we distinguished growth patterns of *Mtb* wild type strain in comparison with the *Rv3218* knockdown (without ATc and with 100 ng/ml ATc) on 7H9 media by conducting growth curves. ATc was added to the culture to mediate the repression of *Rv3218* gene transcription. The PLJR965 plasmid consist of a Tet promoter (Ptet) which controls the binding of RNA polymerase for transcription. When ATc is added, it binds to the Tet promoter, inhibiting the binding of the RNA polymerase which prevents the initiation or the elongation of transcription. Higher concentration of ATc (100 ng/ml) was chosen to ensure the highest efficiency of transcription regulation (Rock *et al.,* 2017).

Growth curves define the cell population density in liquid culture over time, usually obtained by measuring OD of cell populations. Bacterial growth for all the strains showed no statistically significant difference as the p-value results from the t-test showed a p-value greater than 0.05 (p= 0,2). It is quite evident on **figure 3.3.1** that there was no much observable difference in the growth rate of the wild type strain compared to the knockdown strain (with and without ATc), as they reached the stationary phase (OD 600nm of 2) on the same time point (day 13). In the approach taken here, the results are presented in a form of a line graph which consists of OD measurements with respect to time in intervals of 2 days.

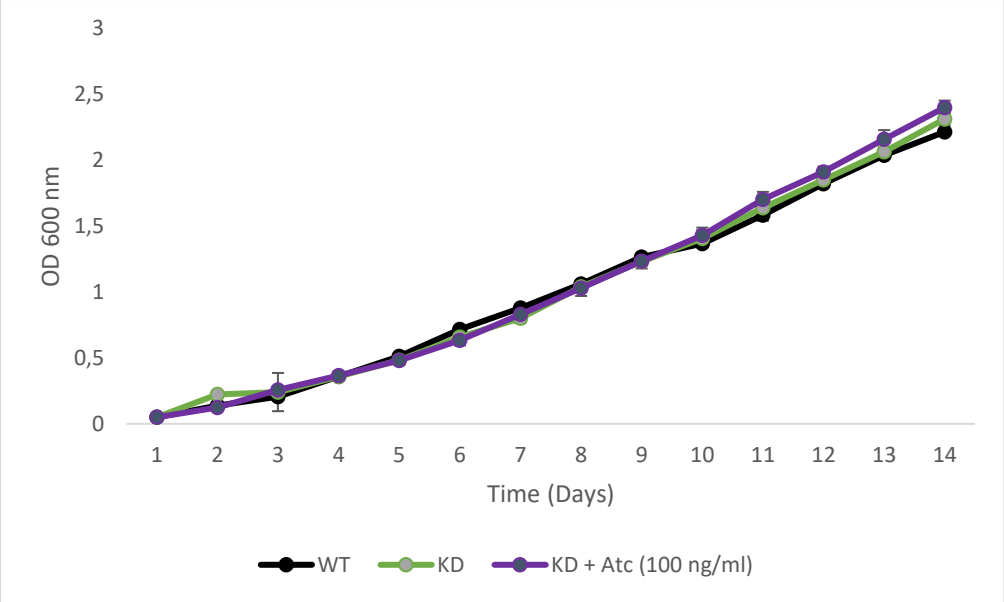

Figure 3.3.1: Growth curves of *Mtb*H37Rv Wild type and Rv3218 Knockdown (KD) with ATc and without ATc, grown on 7H9 media. Each point in the graph is equivalent to the average of three determinants. Error bars were identified using the standard deviation of the triplicate cultures. The black line represents the Wild type, green line represents the *Rv3218* Knockdown without ATc, and the purple line represents the *Rv3218* Knockdown supplemented with 100 ng/ml ATc.

3.4. Minimum Inhibitory Concentrations (MICs)

Inefficiency of medical therapies employed to treat patients infected with bacteria requires not only to actively search for novel therapeutic strategies but also to attentively choose antibiotics based on a number of parameters. Minimal inhibitory concentration (MIC) describes *in vitro* levels of susceptibility or resistance of particular bacterial strains to applied antibiotic. Definitive evaluation of MIC has a crucial impact on the choice of a therapeutic procedure which may affect the coherence of an infection therapy (Kowalska-Krochmal and Dudek-Wicher, 2021). The objective of this study was to determine minimum inhibitory concentrations (MIC) of frequently used antimicrobials for *Mtb* and to evaluate possible differences in MIC between WT and mutants. This was done to check if the silencing or the repression of the *Rv3218* gene will have an impact on the susceptibility of *Mtb* to certain antibiotics.

The strains were tested for antimicrobial susceptibility using broth microdilution. The MIC plate layout showing the different antibiotics used in this study and their concentrations on each well is listed in the appendices section as table 3.1. Antibiotics were chosen with the following objectives; the one that functions in cell wall synthesis, one that inhibits replication, one that inhibits protein synthesis, and one that targets the cytoplasm. Ofloxacin blocks immoderate supercoiling of DNA during replication or transcription, in other words, it inhibits normal cell division (Graham and Tripp, 2022). Meropenem functions in cell wall synthesis by infiltrating through bacterial cells and interfering with the synthesis of crucial cell wall constituents, leading to cell death (Dhillon, 2018). Colistin Sulphate Salts target the cytoplasm by inserting its hydrophobic terminal acyl chain leading to the enlargement of the exterior outer membrane monolayer (Andrade *et al.*, 2020). Erythromycin inhibits protein synthesis simple by binding to the 23S rRNA in susceptible bacteria (Farzam *et al.*, 2022).

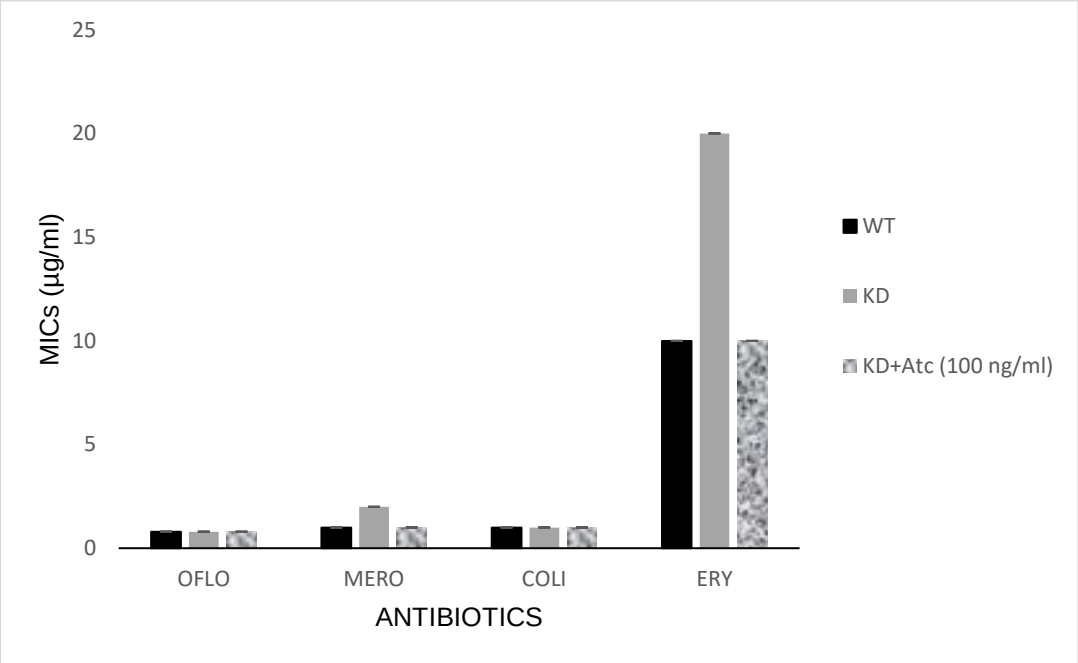

Figure 3.4.1: Graphic representation of the Minimum Inhibitory Concentration of four antibiotics on Wild type vs Knockdown strain (with and without ATc). Error bars were identified using the standard deviation of the triplicate cultures and were plotted on the graph. Oflo: Ofloxacin; Mero: Meropenem; Coli: Colistin Sulphate Salt; Ery: Erythromycin.

From the results illustrated above, we observed that there was no much noticeable difference between the wild type strain and the knockdown strains for Ofloxacin and Colistin sulphate salt, with slight differences in growth of the strains against Meropenem and Erythromycin. The MIC of the wild type strain for Ofloxacin was 0.8 µg/ml which is equivalent to the knockdown strain both with and without ATc. For Meropenem, the wild type and the knockdown strain supplemented with ATc had the same MIC which is 1µg/ml. the MIC values for Colistin sulphate salt was 1µg/ml for all the strains. For Erythromycin, the wild type had the MIC of 10µg/ml, similar to that of the knockdown strain supplemented with ATc. Based on these results, we can suggest that the knockdown of the *Rv3218* has no impact on susceptibility of *Mtb* to the tested antibiotics. The t-test showed no statistically significant differences between the wild type and the knockdown strain as the p value was greater than 0.05 ($p<0.05$).

3.5. Osmolarity Assay

Osmotic stress is among a variety of environmental hazards encountered by microbes throughout the course of contamination (Hatzios *et al.*, 2013). Bacteria have an ability of adapting to exceedingly different microenvironments, but in a number of organisms, the transcriptional programs, signaling pathways, and downstream physiological changes that occur during adaptation are of uncertainty. The bacterial reaction to extracellular signals depend on varied transcriptional regulators (Hatzios *et al.*, 2013).

As *Mtb* continues to cause havoc in public health, understanding of the *Mtb*-host relations is of greater importance as it has a huge potential in revealing novel junctions which can be targeted for diagnostic and therapeutic purposes. The comprehension of the *Mtb*-host interaction can be possible firstly by uncovering the dimensions of the native environment that this microorganism respond to, and also looking at how the basic aspects of *Mtb* biology relate to responses from the environment and success of colonization, (MacGilvary and Kevorkian, 2019). As hypothetical proteins have unknown functions, it can be highly possible that they have major roles in assisting the pathogenic bacteria to survive on different environmental conditions. In this study, *Rv3218* gene is hypothesized to have a diacylglycerol activity. A study by Raetz and Newman, 1977; indicates that strains that bare the dgk mutant do not grow well on media of low osmolarity. To confirm whether the *Rv3218* gene really has a function of

a dgk, we conducted the osmolarity assay where a media with different osmolarity levels was made. Consequently, we cultured *Mtb* H37Rv in Sauton's minimal medium containing 0%, 0.5%, 3%, and 5% (w/v) NaCl for 16 days. These concentrations were chosen because they simulate common hypotonic medium formulations and physiologic concentrations of NaCl encountered in the host niches where *Mtb* resides (MacGilvary and Kevorkian, 2019). For this assay, we firstly had to choose suitable osmolyte and a medium that can be modified to establish different osmolarity conditions. In this case Sauton's minimal media and NaCl were chosen as the media of choice and an osmolyte respectively.

To study the effects of this media on the mutant strains compared to the WT strain, growth curves were conducted and were monitored by OD 600 nm for 15 days. The OD 600 nm was measured against time (24 hrs apart). Shown below are the growth curves from Sauton's minimal media with varying osmolarity (indicated by different NaCl concentrations). The results show that the number of alive cells in Sauton's minimum media supplemented with 0% (**Figure 3.5 A**) and 0.5% (**Figure 3.5 B**) is significantly higher than at other concentrations, which are 3% (**Figure 3.5 C**) and 5% (**Figure 3.5 D**). This result is compatible with previous reports that increased concentrations of Osmolarity by NaCl inhibits the growth rates of other bacterial species (Pang *et al*, 2020). However, according to what the statement says 'the dgk mutants do not grow well in media of slow osmolarity', the results are somehow in disagreement with what is stated. The results show the lowest osmolarity having the highest growth, and the highest osmolarity with the most inhibited growth. No growth difference was observed between the Wild type and the mutant strains in all the concentrations. 3% NaCl shows very slow growth with no growth detected in 5% NaCl.

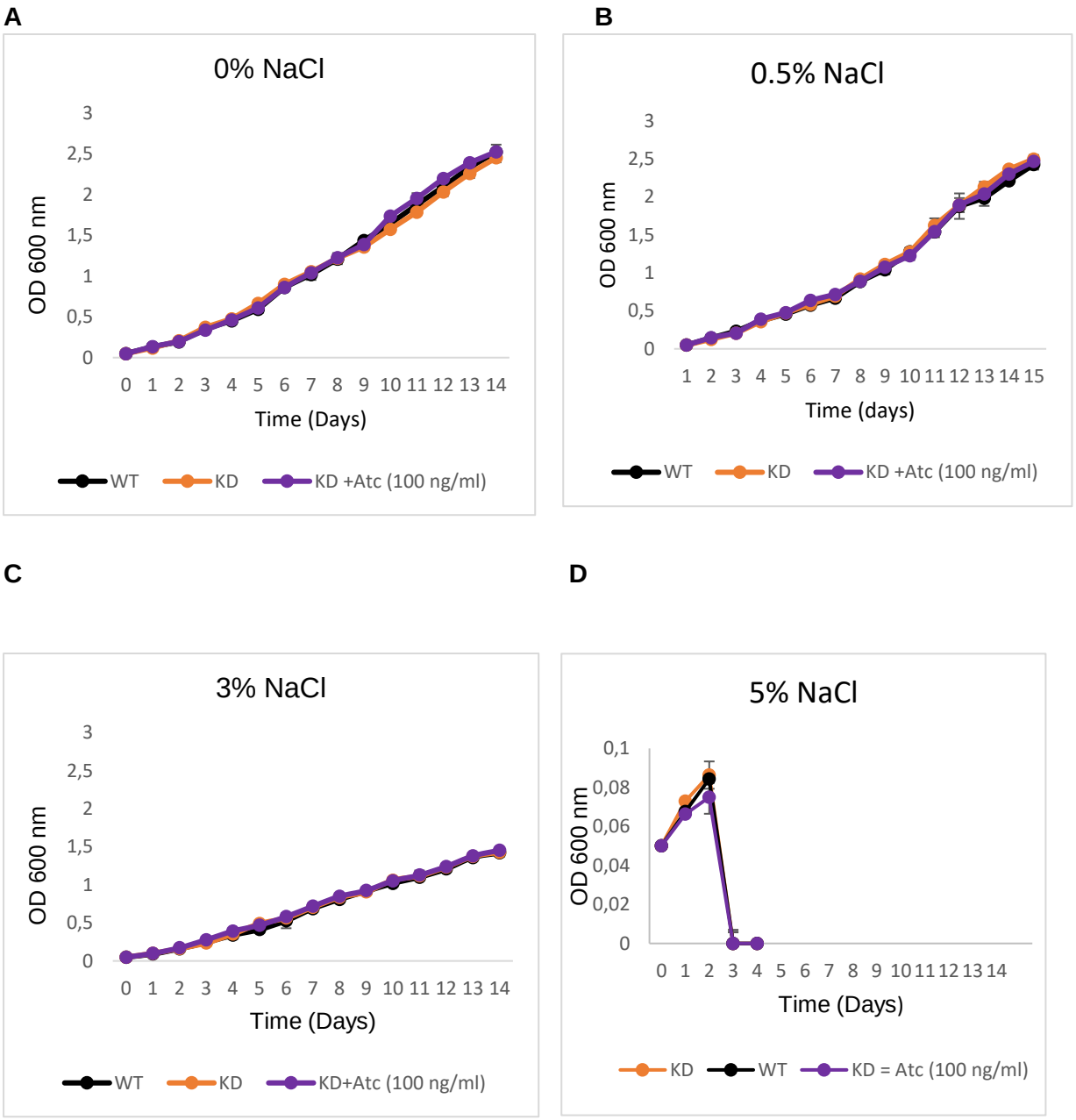

Figure 3.5: Growth of *Mtb* wild type (WT) vs *Rv3218* knockdown (KD) (with and without ATc) on media of different osmolarity adjusted by varying concentrations of NaCl. **A** and **B** show growth of strains in low osmolarity (0% and 0.5% NaCl); **C** and **D** show growth in high osmolarity (3% and 5% NaCl). Each point in the graph is equivalent to the average of three determinants. Error bars were identified using the standard deviation of the triplicate cultures. The black line represents wild type, orange line represents Knockdown (KD) without ATc, and purple line represents Knockdown with ATc.

From these results, it is observable that the knockdown strain (both with and without ATc) is growing similarly with the wild type. No statistical significant difference was found amongst the strains in all osmolarity levels as p value was greater than 0.05 (p=0.1 at 0% NaCl; p=0.09 at 0.5% NaCl; p=0.14 at 3% NaCl; p=0.3 at 5% NaCl). This is in contradiction with the statement that the dgk mutants do not grow well on nutrient media of low osmolarity as there was much abundance of growth on 0% NaCl and 0.5% NaCl which are regarded as of low osmolarity. This can possibly mean that the *Rv3218* gene does not have the dgk activity as low osmolarity did not affect the growth of all the strains.

Chapter 4: Discussion

Mycobacterium tuberculosis (Mtb) is a recurrent bacterium that causes tuberculosis and still persists as a prime pathogen for mortality. This etiological medium of human TB has been identified by Robert Koch for over a century (Chai *et al*., 2018), meaning that a vast amount of time has passed since this discovery and we are still nowhere near close to eliminating this fatal disease (Mishra and Surolia, 2018). As a matter of fact, this infectious agent still continues to be a major drawback for human health. Besides causing TB infection, there is a developing evidence that indicates *Mtb'*s association with numerous other human diseases including autoimmune diseases, pulmonary complications, and metabolic syndromes (Chai *et al.*, 2018).

The emerging of current drug-resistant strains of *Mtb* further complicates the condition, leading to greater difficulties of treatment by regular therapy regimens (Mishra and Surolia, 2018). Humans are the sole reservoir for *Mtb's* existence and dispersion, meaning that it will be much more difficult to eradicate until the extinction of the human race (Mishra and Surolia, 2018). The global consequence of multidrug-resistant TB (MDR TB) is reported by the World Health Organization (WHO) as being a major public health crisis (Sullivan and Amor, 2016). This resistance is caused by *Mtb's* exceptional ability to interfere with the antimicrobial response of the host (Parbhoo *et al*., 2022). This pathogen utilizes detailed tactics to cope with varied host-induced stressors by regulating its physiological state and metabolism for the extension of its survival (Parbhoo *et al.*, 2022).

A variety of genes have different functions that aid at *Mtb's* virulence and survival to different environments. In general, genes are the functional sections of a DNA which have an ability to express themselves and are each responsible for a specific characteristic. Determining the

important genes and predicting their function is of greater significance in assisting with the understanding of *Mtb's* pathogenesis for the successful eradication of this pathogen (Sivashankari and Shanmughavel, 2006). Even though the *Mtb's* genome has been broadly explored for more than two decades, about 27% of its proteins still have no functions assigned to them, and they are annotated as hypothetical proteins (Yang *et al.*, 2019; Silva and, 2020). The genome of any species contains hypothetical proteins that have crucial involvement in several signaling pathways and cellular processes (Naveed *et al.*, 2022). Hypothetical proteins play critical roles in the mechanism of the disease, host adaptation, vaccine production, designing of drugs and production of antibiotics (Naveed *et al.*, 2022).

By understanding the importance of Hypothetical proteins, in the current study, we explored the characterization of the function of the *Mtb* hypothetical protein, the *Rv3218* protein which has a hypothetical function of a diacylglycerol kinase. We first exploited a number of bioinformatics tools for recovering and analysing the gene's biological data in an attempt to assign the function of this protein. On Mycobrowser, we found the size, neighbouring genes, and the location of *Rv3218* in the *Mtb* genome. The location describes the exact position of the gene on the chromosome. Knowing the location also made it feasible to determine the closest genes that are already annotated. The significance of analysing the physicochemical variables of hypothetical proteins is mainly useful in the transition from the *insilico* analysis to *in vitro* studies (Silva *et al.,* 2020). For example, knowing the isoelectric point of a protein will make it possible to adjust the pH for experimental analysis of the given protein (Silva *et al.*, 2020) and knowing the gene length can be essential for the construction of a recombinant DNA plasmid. From the *insilico* analysis, we also found that the *Rv3218* protein shares a variety of similarities and traits with the Diacylglycerol kinase, including the domains, interactions, and protein structures as well as belonging to the same superfamily of kinases. This led to high possibilities that the *Rv3218* gene is a diacylglycerol kinase with cell wall functions, particularly lipid biosynthesis. Diacylglycerol kinases, located in the plasma membrane (Van Horn and Sanders, 2012), are large members of a conserved and distinctive family of intracellular lipid kinases that function in the catalysis of the conversion of Diacylglycerol into phosphatidic acid (Merida *et al.*, 2008). Phosphatidic acids are connected to a variety of functions in the cell wall, including membrane trafficking, cell growth, migration and differentiation (Wattenberg and Raben, 2007; Merida *et al*, 2008).

There are several studies that focused at characterising the functions of hypothetical proteins in *Mtb* via gene deletion. These studies include a study by Owens *et al.,* who proved that *Mtb*

Rv2252 encodes a diacylglycerol kinase involved in the biosynthesis of phosphatidylinositol mannosides (PIMs) (Owens *et al*., 2006). In the present study, to prove that the *Rv3218* is a diacylglycerol kinase, we exploited a CRISPRi dcas9 molecular system to construct a targeted gene knockdown in *Mtb* for *in vitro* analysis of the *Rv3218* gene. CRISPRi focuses on mediated repression of transcription by a (Ptet) dcas9 inducible by Anhydrotetracycline (ATc), which is directed to the specific DNA targets by an ATc-inducible expressed sgRNA, which prevents transcription initiation or elongation (Rock *et al.*, 2017). There is a variety of published studies that have shown successful transcription repression using the CRISPRi dCa9 system which include repression in *E, coli* (Tong *et al.*, 2021), *Staphylococcus aureus* (Penewit and Salipantse, 2020), and *Acitenobacter baumanni* (Wang *et al*., 2019). However, the system has some major shortcomings which include the partial or incomplete inactivation of the gene of interest and potential off-target effects (Karlson *et al*., 2021). Our results suggest that our attempt to construct a gene knockdown was successful, the sgRNA 20-nt base-pairing region was able to bind to the target DNA by complementary base pairing and to the dcas9 via the dcas9 handle site leading to the formation of the sgRNA-dcas9-DNA complex (Myrbråten *et al.*, 2019). This is consistent with several findings from other studies that used the CRISPRi system for gene silencing, including the study by Choudnay *et al.*, where they constructed a CRISPRi system for gene silencing in mycobacteria for the characterization of essential genes in the mycobacterial genome.

To test the effect of the repressed transcriptional expression of the *Rv3218* gene on growth and survival of *Mtb*, we firstly conducted growth curves for the analyses of the growth patterns on the wild type strain compared to the *Rv3218* knockdown strain. This was done to observe differences in growth of *Mtb* when the *Rv3218* gene is suppressed in comparison with the *Mtb*H37Rv wild type. Our growth curve results show that the knockdown strains were growing at the same rate as the wild type. The statistical analysis did not show any significant difference among the strains. This means that this mutation did not interfere with the critical growth properties which may include the utilization of essential carbon or nitrogen sources necessary for growth (Hibbing *et al.*, 2010). This can imply that the *Rv3218* gene can be classified under non-essential genes as growth was not inhibited under its repressed transcription (Fang *et al.*, 2005). However, this contradicts the findings from Mycobrowser which denoted that this gene has cell wall and transcriptional functions.

After conducting growth curves, we then performed biological assays to investigate and analyse the function of *Rv3218* gene. We conducted antimicrobial susceptibility testing (MICs)

to test the effect of the *Rv3218* gene knockdown on *Mtb* comparing susceptibility of the wild type strain to the knockdown strains. The MICs were conducted to test if this hypothetical protein plays an important role in *Mtb* drug resistance since it is stated that some hypothetical proteins may possibly play crucial roles in disease progression and survival of the pathogens (Gazi *et al.,* 2018). Antimicrobial susceptibility testing is a crucial step in the development of effective and efficient treatment regimens (Getahun *et al.,* 2022). For obtaining the proper MIC results, we considered some few elements including proper method choice, precise adherence to labelling rules, and adequate interpretation of the results (Kowalska-Krochmal and Dudek-Wicher, 2021). The MICs of Ofloxacin, Meropenem, Colistin sulphate salt and erythromycin, were determined against *Mtb* strains (wild type and knockdown) by the standard broth microdilution methods on microtiter plates using antibiotic concentrations ranging from 0.02-25.6 µg/ml for Ofloxacin, 0.12-128 µg/ml for Meropenem, 0.03-32 µg/ml for Colistin Sulphate Salt, and 0.12-160 µg/ml for erythromycin. This method of susceptibility testing was chosen because of numerous advantaged including faster reporting of results as compared to other methods, and the microtiter plates method is much easier to set up and provides accurate reading of results (Hall *et al.,* 2011). The MICs were delineated as the lowest concentrations at which no visible turbidity was observed (Shandil *et al.,* 2006; Kowalska-Krochmal and Dudek-Wicher, 2021). Our findings suggest that the silencing of the *Rv3218* gene showed no pivotal impact in the antimicrobial susceptibility of *Mtb* against all the antimicrobials that were tested in this study as there was no significant differences on the MIC results of the knockdown as compared to the wild type strain. The results also suggest that this gene does not play major roles in antimicrobial susceptibility of *Mtb* to these antimicrobials.

The understanding of the bacterial factors that mediate the survival of *Mtb* in the host environment is a challenge to our understanding of mycobacterial pathogenesis (Owens *et al.,* 2006). Throughout the *Mtb's* cycle of infection, *Mtb* experiences and lives in distinct environments within the human body including nutrient deficient, nitrosative, acidic, and hypoxic niches, instituted both extracellularly and intracellularly. It also experiences different osmolar and electrolyte stresses (Larrouy-Maumus *et al*., 2016; Fen Li *et al*., 2021). Osmotic stress is a physiological debilitation formed by an unexpected alteration in the concentration of the solutes around a cell which leads to a swift change in the motion of water across its cell membrane (Csonka, 1989). The deeper understanding of how microbes perceive and counter act to the changes in extracellular osmolarity is still not clear (Hatzios *et al.,* 2013), although it

is said that osmotic variations change the turgor pressure which can damage metabolic activity and protein folding.

In this study, we followed a statement by (Raetz and Newman, 1977) that states that dgk mutants do not grow well on nutrient media of low osmolarity. As dgk leads to the synthesis of high amount of lipids, it makes it hard for the cell wall to absorb enough solutes that are essential for growth. Low osmolarity media means not enough solutes. Cell wall rich in lipids needs more solutes that will serve as emulsifiers to break down the lipids to allow for more nutrient absorption necessary for growth (Escorbar *et al.*, 2017). Our attention on osmotic stress was also persuaded by the fact that *Mtb* has the great abilities to adjust to different changes in osmolarity of the environment as it moves between mucosal epithelia, airborne droplei nuclei, alveolar macrophages, caseous granulomas, and mecrotic cells (Hatzios *et al.*, 2013). As *Rv3218* is hypothesized to have a dgk activity, we sought to develop an osmolarity assay to check if there'll be any difference in the growth of *MtbH37rv* strain in comparison with the *Rv3218* knockdown strain.

The osmolarity of Sauton's minimal media was adjusted by adding NaCl to final concentrations of 0%; 0.5%; 3%, 5% (w/v), with the notion that the higher the NaCl concentration, the higher the osmolarity. NaCl has been used in a number of published studies to adjust osmolarity of a nutrient media including a study by (François Gagné, 2014); (Schwan *et al,* 2002) and (Rebollo-Ramirez and Larrouy-Maumus, 2019). We conducted growth curves of *Mtb* Wild type and mutant strains for all the concentrations of NaCl. We observed that the highest osmolarity (5%) resulted in the inhibition of the growth of all the strains, with 3% showing very slow growth. This may be due to the fact that the cell envelope composition is greatly affected by drastic changes in osmolarity (Larruoy-maumus, 2019). The cell envelope functions in cell protection, cell interactions with the environment, and most importantly, cell growth (Holst *et al*, 2009). Any distraction to the cell envelope interrupts the state of cell electrolytes, which can then lead to the activation of death pathways such as apoptosis (Silhavy *et al.*, 2010). We also found that the number of viable cells in Sauton's minimal media supplemented with 0% and 0.5% NaCl (low osmolarity) was remarkably higher than on other tested osmolarity levels. This may be as a result of *Mtb's* Peptidoglycan structure that forms a strong, hard layer exterior the plasma membrane permitting the bacterium to withstand the consequences of changes in different osmotic pressure (Angala *et al.*, 2014; Pavelka *et al.*, 2014). These findings are similar to the findings by Rebollo-Ramirez and Larrouy-Maumus,

2019, where they were characterizing the response of *Mtb* to osmotic stress using physiological varies of NaCl. They also found that as osmolarity levels increase, the more the *Mtb* growth is inhibited. The results are also compatible with the preceding reports that showed the elevated osmolarity levels inhibit growth patterns of most if not all bacterial species (Schwan *et al.*, 2002). This can be due to the fact that fluctuations in osmolarity change the turgor pressure which then leads to the impairment of metabolic activity and protein folding (Hatzios *et al.*, 2013; Auer and Weibel, 2017).

CONCLUSION

In sum, we constructed an *in vitro* assembled dCas9/sgRNA system to silence *Rv3218* gene in order to characterize its function in *Mycobacterium tuberculosis*. The gene is hypothesized to have a diacylglycerol kinase activity. First and foremost, it can be taken into consideration that hypothetical proteins do not have enough published data that can assist in their study and research. In this study, the findings provide the first evidence of Growth curves, MICs, and osmolarity experiments conducted on the *Rv3218* gene. These experiments have shown that the *Rv3218* gene has no impact on the growth of *Mtb* and no impact on the antimicrobial susceptibility of *Mtb* to the antimicrobials that were used in this study. Our findings also suggest that the *Rv3218* gene does not act as a diacylglycerol kinase as it is hypothesized to be. However, before concluding that this gene does not act as hypothesized, we suggest that more advanced studies; that may include the use of a gene knockout where a gene is completely deleted rather than silenced; still need to be conducted in order to confirm the hypothesis as we could not do them due short time frames.

APPENDICES

Appendix A: Culture media:

Nutrient Broth (NB):

15g nutrient broth powder, 1000 ml sdH20

Middlebrook 7H9:

4.7 g Difco Middlebrook 7H9 powder, 2 ml glycerol, 900 ml dH2O, 10 ml 100X glucose-salt, 2 ml Tween80

Middlebrook 7H11:

19 g Difco Middlebrook 7H11 powder, 5 ml glycerol, 900 ml dH2O, 10 ml 100X glucose-salt

Sauton's minimal media (pH 7.2):

4 g asparagine, 0.5 g magnesium sulphate, 2 g citric acid, 0.5 g potassium dihydrogenorthophosphate, 0.05 g ammonium ferric citrate, 48ml glycerol then sterilized by filtration.

NZY^+ broth:

10 g NZ amine (casein hydrolysate), 5 g yeast extract, 5 g NaCl, 1 litre dH_2O, (pH 7.5 adjusted using NaOH then autoclaved). Add filter-sterilized 12.5 ml of 1 M $MgCl_2$, 12.5 ml of 1 M $MgSO_4$, 10 ml of 2 M glucose.

Tween80 (25 %):

10 ml Tween80 dissolved in 40 ml dH2O then sterilized by filtration

Appendix B: Solutions

DNA manipulation solutions:

1 M Tris-HCl : 60.56 g Tris, pH 8.0 with HCl, 500 ml dH2O final volume

0.5 M EDTA : 18.6 g powder, pH 8.0 with NaOH, dH2O

Soln I : 50 nM glucose, 25 mM Tris-HCl, 10 mM EDTA, pH 8.0

Soln II : 0.2 M NaOH, 1.0 % SDS

Soln III : 5 M potassium acetate, 11.5 ml glacial acetic acid, 88.5 dH20, pH 4.8

Sodium Borate Buffer: 47 g Boric Acid, 8 g Sodium Hydroxide, 1000 ml sdH20

Chloroform: Isoamyl alcohol : 24 ml chloroform, 1 ml isoamyl alcohol

Phenol: chloroform : 1 ml phenol, 1 ml chloroform

Sodium acetate : 3M sodium acetate dissolved in dH2O (autoclaved)

CTAB/NaCl : 4.1 % NaCl, 10 % N-cetyl-N, N, N-trimethyl ammonium bromide dissolved in dH2O (filter sterilized)

Appendix C: Molecular weight markers

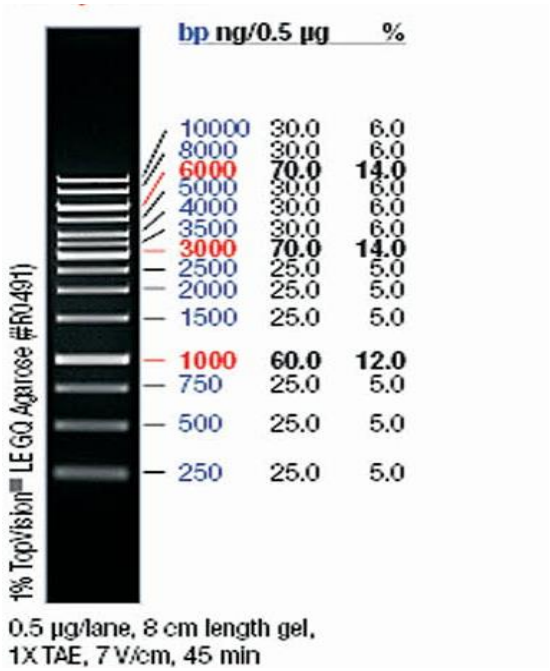

1 Kb GeneRuler

Appendix D: Bioinformatics analysis:

Rv3218 gene sequence from Mycobrowser:

gggcccggaagctgcctgactggccgaccggcccgctgcccaaggtacgcgtcgccgccgcccttccg
ccacctgccgactacctgacccggatcggccgcgcacgggatctgctggccgccttcgacggcccgtt
gcacaaagtggtgctcgcgcgccgtgcaactgaccgccgatgctccgctggacgcgcgggtactgt
tgcgcaggttggtcgtcgccgacccgaccgcttacggctatctcgtcgacctcacctctgcgggcaac
gacgacaccggggcagccctggtcggcgccagcccagagcttctggtcgcacgatccggcaatcgcgt
catgtgcaagccatttgccggctcagccccacgcgccgccgaccccaaactcgacgccgccaacgcgg
ccgcactagccagttcggccaagaaccgacacgaacaccaattggtcgtcgacacgatgcgggtagcc
ctagagccactatgcgaggacctgacaatcccagcccagccccagttgaaccgcaccgcagccgtttg
gcatctgtgcaccgcgatcaccggccggctgcgcaacatctcgacgacggcaatcgatctggctttgg
cgctacatcccacccccggcggttggtggggtcccgacaaaagctgccaccgagctcatcgccgaactc
gagggcgaccgtggcttctacgccggcgcggttggttggtgcgacggccggggcgacggccattgggt
ggtgtctatccggtgcgcgcaactttcggctgatcgacgcgcagcccttgcgcacgctggcggtggca
tcgtcgccgaatcagaccccgatgacgaacttgaagaaaccacaacgaagttcgccacgatattgacc
gcactgggagttgagcagtgaccgataccatccgccgcgctacaccggcggataccgccgacatcgtg
gccatgattcacgcgctgggcggaattcgagtatgccgccgatcaatgcactgtcaccgaaacacaaa

tacatacagcacttttcggagatttcccgacgatgcgaggccacgtcgctgaggttaatggcggagtt
gccgcgatggcgctgtggtttctgaacttttccacctgggacggcgtcgcgggcatctatgtggagga
cttgttcgtctggccgaggtttcgccgccgcggcttggcccgtggcctgctgtcgacgctggccagag
aatgcgtcgacaaccgctacacgcggttggcctggtcggtgctgaactggaattccgatgcaatcgca
ctgtatgaccgcatcggcgggcaaccgcagcacgagtggactatctatcgactgtcaggaccgcggtt
ggctgcgctggccgcaccacgctgatcacgcccggcggcccagcggatcgaaggcggactgaacagca
ataccagcacgccaagcgcgatgattcccaccgggatcccgatcgccggctgatgcgaacccacaatc
agataccacgccaccggcagcagcagcagctgggcgaacaccgccagcccgcgaccccaaagcttgcc
aaccgccagcctgcatccggcggcgagcactgctccgccgaccagtacgaaccaacctgcggtgccca
ggccattgacgatgtgctggtcggcgcccgcgagtccgcgcaccagcaacgccgcggccaccaccagg
gcggccccaccctgcacggcgacgatcagtccggcgccgcgcacggcggccggggctcgaacaggcac
agcatcagcgtagtcacccggccgtgaccggcccgcatcgtcacaccacccaggcccattgccgtcct
cctcaacgggccgacccggcccgcatcgtcacacggcctaggcccattgccgtcctcctcaacgggcc
gacccggcccgcatcgtcacacggcctaagcccattgccgtcctcctcaacgggccgacccggcccgc
atcgtcacacggcctaagctcgtgcgtcatgcgtgcagtgctgatcgtcaaccccactgcgaccgcca
ccacaccagccggccgcgacctgctggcgcacgccctcgaaagccgccttcagctcacggttgagcac
accaaccaccgcggtcacgggaccgaactcggacaggcggcggtagccgacggggtggacctggtcgt
ggtgcatggcggcgatggcacggtaagcgccgtagtcaacggcatgctggggcgccccggcacgacgc
cggtccgaccggtgccagccgttgcggttgtgcccggcggctcggccaacgtactagctcgcgcgcta
gggatttccgcggacccgatcgctgccaccaaccaactcatccagctgctcgacgactacggccgcca
ccagcagtggcgccgcatcgggctgatcgactgcggtgagcggtgggcggtgttcaacgccggcatgg
gcgtcgacgccgaggtcgtggccgcggtagaggccgaacgcgacaaaggcggcaaggttacggcgtgg
cgctatattcgcgctgcggtgcgcgcggtgctcgcctgcactcgtcgcgaaccggctcttacgctgca
acttcccaaccgcgatccaattaccggagtgcactttgtgttcgtgtccaactccagtccgtggactt
acgcaaacaaccggccggtatggaccaatcccgactgcaggttcgagtcggggctgggagtgttcgcc
accaccagcatgaaggtggtcccgaccctgagggtggttcggcagatgttcgcaaaacagcccaagtt
cgagttcaaccacgtcatcaacaacgacgacgtcgcgtgtctacgcgtcacctccatggggcccccga
tcgccagccaattcgacggggactacctcggcgtgcgcgagacgatgacgttccgagctgttcccgac
gccctcgccgtagttgccccgcccgcaagaaagcggatctgagctgcagaaacaaagatgtgatgggt
gtgcgacacaaacgttgggcgaaactggcagcgtagtgtagtacaactgggtaagggctgtggaacga
gatcgccagagtgagatagcccacgcgcttacgtaacactattgacatctgttgagcctgtgaaacga
tcaaaaggttgcatgtagagaaatgtaggggtacagaagcctttcttgtgcacccgttaccagccaag
aagaaacgcctgtgcgtaccgctgcgcacatagtgaggagtaacgactaatggattggcgccacaagg
cggtctgtcgtgacgaggatccggaactgttcttcccggtaggaaacagtggtccggcacttgcgcag
atcgctgacgcgaaactggtctgtaatcggtgcccggtcaccacagagtgcctcagctgggcactgaa
taccggccaggactcgggcgtctggggaggcatgagcgaagacgagcggcgcgcgctgaagcgtcgca
acgcccgcacgaaagcccgtaccggggtctgacgactcagttctgcacagtgcggccccgacatacgt
cggggccgcactgttgcgtagcgcgctacagcatcaaccgtccccggcgtccgaccggtacccgtagc
accacatcggtgccacgttcgcgggcgtcccgcatacctaacgagccgtccaattccgcagagaccaa
ggtccgcacgatctgcaggcccaggctgtccgacttctccaggctgaaaccttgcggcagaccaagcc
cgtcgtcgtgcacgacgacatcgagccaacgcgcagagcgttccgctcgaatcgtcacggacccttcc
gccgccgccgggtcgaacgcatgctcgatcgcgttctgcaccagctcggtgatcaccatgatcagcgc
cgtggcgcggtcggagtcgagcacaccgaggtcgccaacccgatttatccggatcggcctgtccaccg
atgccacatcgttcatgatcggcagaatccggtcgatgacctcgtcaaggttcacctgctcgtccacc
gacatcgacaacgcatcgtggaccaaggcaatcgacgacactcggcgcaccgactcgatcagcgcttc
ccgcccctcggcgttggacgtccggcgagcctgcagccgcaacagcgcggccaccgtctgcaggttgt
tcttaacccgatgatggatttcccggatcgtggcgtccttggatatcagggctcggtcgcgccgcttc
acctcggtcacgtcgcggatcaatatcgcggcgccgacattgcgaccagctaccaccagcggcagagt
ccgcagcagcaccgtggcgccgccggcgtcgacctccatccgcatacccttccatccccggccagca

agtcctgcacatgctcgtctacctcgtgcgcctcgaacgggtccgagatcagcgggcgcgtcgcgtca
atgagattgacgccctccaactcggtggtcaaacccattcggtggtaagccgatagggcattggggct
ggcgtaagagaccacaccgtcgacatcgagacggatgaagccgtcacccgcgcgcgggctagatcgcg
acatcgccacgtcccctgcgtcgggaaaggtgccctccgccagcatccggagaagatctgtggcgcac
aaccgataggcggtctccaggtggccggatctacgtcgcgccgccagttcgggttgatgccgtgtcag
caccgccaccacctgatcgccaaagcgcaccggggagacttcgacactgtggccgtcgtgttgacatg
aattctgttggccgacagcgccttcccgtcccgggacaccaccggagaaggtcgcggcgaccagcggc
atgctattggcggcgacgacggtgcctaccgcgtcggtatgcaccaccgtcggcccggtgttcggccg
gcattgcgcaacgcacaccaggacaccgtcgtcgcggcgaacccacatcaggtaatcggcaaacgaca
ag

Rv3218 protein sequence from Mycobrowser:

MRAVLIVNPTATATTPAGRDLLAHALESRLQLTVEHTNHRGHGTELGQAAVA
DGVDLVVVHGGDGTVSAVVNGMLGRPGTTPVRPVPAVAVVPGGSANVLARA
LGISADPIAATNQLIQLLDDYGRHQQWRRIGLIDCGERWAVFNAGMGVDAEV
VAAVEAERDKGGKVTAWRYIRAAVRAVLACTRREPALTLQLPNRDPITGVHFV
FVSNSSPWTYANNRPVWTNPDCRFESGLGVATTSMKVVPTLRVVRQMFAKQ
PKFEFNHVINNDDVACLRVTSMGPPIASQFDGDYLGVRETMTFRAVPDALAV
VAPPARKRI

In silico ligation of *Rv3218* sgRNA and PLJR965 plasmid on Clone manager:

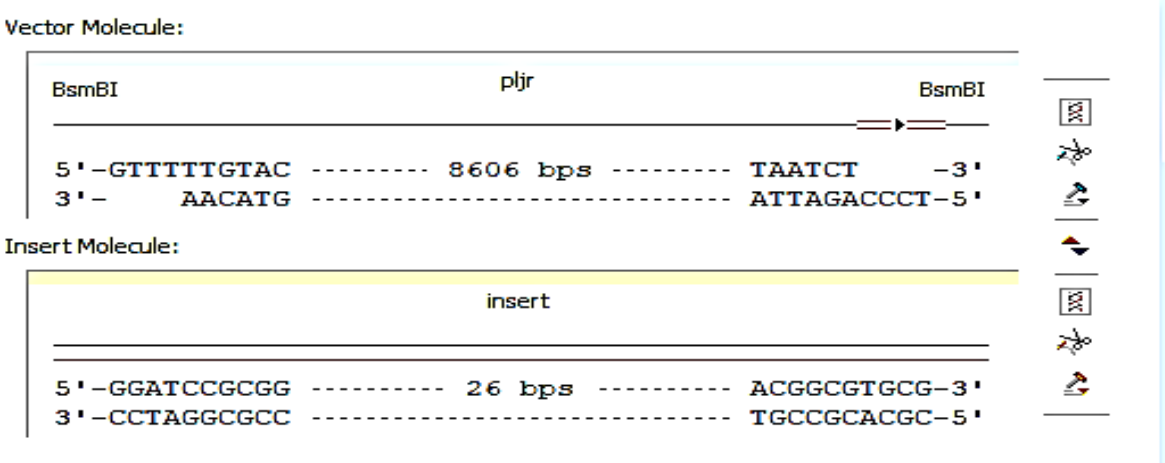

Appendix E: additional information:

Table 3.1. MIC table representing a Microtiter plate layout for Wild type and Knockdown strains.

	Concentrations (µg/mL)									
Drugs	1	2	3	4	5	6	7	8	9	10
Ofloxacin	25.6	6.4	3.2	1.6	0.8	0.4	0.2	0.1	0.05	0.02
Meropenem	128	32	16	8	4	2	1	0.5	0.25	0.12
Colistin Sulphate Salt	32	8	4	2	1	0.5	0.25	0.13	0.06	0.03
Erythromycin	160	40	20	10	5	2.5	1.25	0.63	0.32	0.12

Table 3.2: MIC tabulated results

Strain	Antibiotic	MICs (µg/ml)
WT	Oflo	0.8
	Mero	1
	Coli	1
	Ery	10
KD without ATc	Oflo	0.8
	Mero	2
	Coli	1
	Ery	20
KD+ ATc (100 ng/ml)	Oflo	0.8
	Mero	1
	Coli	1
	Ery	10

Appendix F: Ethics approval

UNIVERSITY OF KWAZULU-NATAL
INYUVESI YAKWAZULU-NATALI

25 June 2020

Miss Khumbuzile Canham (220061969)
School of Lab Med & Medical Sc
Medical School

Dear Miss Canham,

Protocol reference number: BREC/00001516/2020
Project title: characterizing the function of the Rv3218 gene in Mycobacterium tuberculosis
Degree Purposes: MMedSci

EXPEDITED APPLICATION: APPROVAL LETTER

A sub-committee of the Biomedical Research Ethics Committee has considered and noted your application.

The conditions have been met and the study is given full ethics approval and may begin as from 25 June 2020. Please ensure that outstanding site permissions are obtained and forwarded to BREC for approval before commencing research at a site.

This approval is subject to national and UKZN lockdown regulations dated 5th June 2020 which is available on the BREC website (http://research.ukzn.ac.za/Libraries/BREC/Proposed_UKZN_BREC_revision_to_research_constrains_anticipating_change_to_Level_3_lockdown.sflb.ashx).

This approval is valid for one year from 25 June 2020. To ensure uninterrupted approval of this study beyond the approval expiry date, an application for recertification must be submitted to BREC on the appropriate BREC form 2-3 months before the expiry date.

Any amendments to this study, unless urgently required to ensure safety of participants, must be approved by BREC prior to implementation.

Your acceptance of this approval denotes your compliance with South African National Research Ethics Guidelines (2015), South African National Good Clinical Practice Guidelines (2006) (if applicable) and with UKZN BREC ethics requirements as contained in the UKZN BREC Terms of Reference and Standard Operating Procedures, all available at http://research.ukzn.ac.za/Research-Ethics/Biomedical-Research-Ethics.aspx.

BREC is registered with the South African National Health Research Ethics Council (REC-290408-009). BREC has US Office for Human Research Protections (OHRP) Federal-wide Assurance (FWA 678).

The sub-committee's decision will be noted by a full Committee at its next meeting taking place on 14 July 2020.

Yours sincerely

[redacted]

Prof D Wassenaar
Chair: Biomedical Research Ethics Committee

Biomedical Research Ethics Committee
Chair: Professor D R Wassenaar
UKZN Research Ethics Office Westville Campus, Govan Mbeki Building
Postal Address: Private Bag X54001, Durban 4000
Email: BREC@ukzn.ac.za
Website: http://research.ukzn.ac.za/Research-Ethics/Biomedical-Research-Ethics.aspx

References

Advani, J., Verma, R, Chatterjee, O., Pachouri PK, Upadhyay P, Singh R, Yadav J, Naaz F, Ravikumar R, Buggi S, Suar M, Gupta UD, Pandey A, Chauhan DS, Tripathy SP, Gowda H, & Prasad TSK. (2019). Whole Genome Sequencing of *Mycobacterium tuberculosis* Clinical Isolates From India Reveals Genetic Heterogeneity and Region-Specific Variations That Might Affect Drug Susceptibility. *Front Microbiol*. 26;10:309.

Ahsan, M.J. (2015). Recent advances in the development of vaccines for tuberculosis. *Ther Adv Vaccines.* 3(3):66-75.

Alderwick, L.J, Harrison, J., Lloyd, G.S, & Birch, H.L. (2015). The Mycobacterial Cell Wall-Peptidoglycan and Arabinogalactan. *Cold Spring Harb Perspect Med.* 27;5(8):a021113.

Al-Saeedi, M & Al-Hajoj S. (2017). Diversity and evolution of drug resistance mechanisms in *Mycobacterium tuberculosis*. *Infect Drug Resist*. 13;10:333-342.

American Lung Association. (2020). Treating and managing Tuberculosis.

Andrade, F.F, Silva, D., Rodrigues, A., & Pina-Vaz C. (2020). Colistin Update on Its Mechanism of Action and Resistance, Present and Future Challenges. Microorganisms. 2;8(11):1716.

Andrews, J.M. (2001). Determination of minimum inhibitory concentrations. *J Antimicrob Chemother.* 1:5-16.

Angala, S.K, Belardinelli, J.M, Huc-Claustre, E., Wheat, W.H, & Jackson M. (2014). The cell envelope glycoconjugates of Mycobacterium tuberculosis. *Crit Rev Biochem Mol Biol*. 361-99.

Auer, G.K., & Weibel DB. (2017). Bacterial Cell Mechanics. *Biochemistry*. 56(29):3710-3724.

Barberis, I., Bragazzi, N.L., Galluzzo, L., & Martini, M. (2017). The history of tuberculosis: from the first historical records to the isolation of Koch's bacillus. *J Prev Med Hyg*. 58(1):E9-E12.

Basu, M.K., Poliakov E, & Rogozin IB. (2009). Domain mobility in proteins: functional and evolutionary implications. *Brief Bioinform*. 10(3):205-16.

Bateman, A., Coggill, P., & Finn, R.D. (2010). DUFs: families in search of function. Acta Crystallogr Sect F Struct Biol Cryst Commun. 1;66(Pt 10):1148-52.

Baumschlager, A., Rullan, M., & Khammash, M. (2020). Exploiting natural chemical photosensitivity of anhydrotetracycline and tetracycline for dynamic and setpoint chemo-optogenetic control. *Nat Commun*. (1):3834

Beloor, S.A, Rosani, A., Wadhwa, R. (2022). Rifampin. In: *StatPearls. Treasure Island*

Bendre, A.D., Peters P.J., & Kumar J. (2021). Tuberculosis: Past, present and future of the treatment and drug discovery research. *Curr Res Pharmacol Drug Discov*., 2 10.1016

Bray, J.E., Todd A.E., Pearl F.M.G., Thornton J.M., & Orengo C.A. (2000). The CATH Dictionary of Homologous Superfamilies (DHS): a consensus approach for identifying distant structural homologues, *Protein Engineering, Design and Selection*, 153–165

Camus, J.C., Pryor, M.J., Médigue, C., & Cole S.T. (2002). Re-annotation of the genome sequence of *Mycobacterium tuberculosis* H37Rv. *Microbiology* 2967-2973.

Carroll, P., Muttucumaru D.G., & Parish T. (2005). Use of a tetracycline-inducible system for conditional expression in *Mycobacterium tuberculosis* and *Mycobacterium smegmatis*. *Appl Environ Microbiol*. 71(6):3077-84.

Chai, Q., Zhang Y., Liu C.H. (2018). *Mycobacterium tuberculosis*: An Adaptable Pathogen Associated With Multiple Human Diseases. *Front Cell Infect Microbiol*. 15;8:158.

Che, Y., Bo, D., Lin, X(2021). Phenotypic and molecular characterization of pyrazinamide resistance among multidrug-resistant *Mycobacterium tuberculosis* isolates in Ningbo, China. *BMC Infect Dis* **21**, 605

Chiliza, T.E., Pillay, M., Naidoo, K. & Pillay, B. (2019). Immunoscreening of the M. tuberculosis F15/LAM4/KZN secretome library against TB patients' sera identifies unique active- and latent- TB specific biomarkers. *Tuberculosis (Edinb).* 115:161-170.

Chiaradia, L., Lefebvre, C., Parra, J. *et al.* Dissecting the mycobacterial cell envelope and defining the composition of the native mycomembrane. *Sci Rep* **7**, 12807 (2017). https://doi.org/10.1038/s41598-017-12718-4

Choudhary, E., Thakur, P., & Pareek, M. (2015). Gene silencing by CRISPR interference in mycobacteria. *Nat Commun* 6, 6267

Cole, S., Brosch, R., Parkhill, J. *et al.* (1998). Deciphering the biology of *Mycobacterium tuberculosis* from the complete genome sequence. *Nature* **393**, 537–544

Cole, S.T. (1999). Learning from the genome sequence of *Mycobacterium tuberculosis* H37Rv. *FEBS Letters*, 1–2.

Cook, G.M., Berney, M., Gebhard, S., Heinemann, M., Cox, R.A., Danilchanka, O., & Niederweis, M. (2009). Physiology of mycobacteria. *Adv Microb Physiol*., 318-9.

Csonka, L.N. (1989). Physiological and genetic responses of bacteria to osmotic stress. *Microbiol Rev*. 121-47.

Daffé, M., & Etienne, G. (1999). The capsule of Mycobacterium tuberculosis and its implications for pathogenicity. *Tuber Lung Dis*. 79(3):153-69.

Dlatu, N., Longo-Mbenza, B., & Apalata T. (2022). Predictors of tuberculosis incidence and the effects of multiple deprivation indices on tuberculosis management in OR Tambo district over a 5-year period. *PLoS ONE* 17(3): e0264811.

Dartois, V.A., & Rubin, E.J. (2022). Anti-tuberculosis treatment strategies and drug development: challenges and priorities. *Nat Rev Microbiol* **20**, 685–701

Daugelat, S., Kowall, J., Mattow, J., Bumann, D., Winter, R., Hurwitz, R., Kaufmann, S.H.E. (2003). The RD1 proteins of *Mycobacterium tuberculosis*: expression in *Mycobacterium smegmatis* and biochemical characterization. *Microbes and Infection*, 1082-1095,

Delogu, G., Sali, M., & Fadda, G. (2013). The biology of *mycobacterium tuberculosis* infection. *Mediterr J Hematol Infect Dis*. 16;5(1):e2013070.

Dhillon, S. (2018). Meropenem/Vaborbactam: A Review in Complicated Urinary Tract Infections.. *Erratum in: Drugs*. 78(12):1259-1270

Diacon, A., Miyahara, S., Dawson, R., Sun, X., Hogg, E., Donahue, K., Urbanowski, M., De Jager, V., Fletcher, C.V., Hafner, R., Swindells, S., & Bishai, W. (2020). Assessing whether isoniazid is essential during the first 14 days of tuberculosis therapy: a phase 2a, open-label, randomised controlled trial. *Lancet Microbe*. (2):e84-e92..

Doerks, T., van Noort, V., Minguez, P., & Bork, P. (2012). Annotation of the *M. tuberculosis* hypothetical orfeome: adding functional information to more than half of the uncharacterized proteins. *PLoS One*. 7(4):e34302.

Escobar-Sepúlveda, H.F., Trejo-Téllez, L.I., Pérez-Rodríguez, P., Hidalgo-Contreras, J.V., & Gómez-Merino, F.C. (2017). Diacylglycerol Kinases Are Widespread in Higher Plants and Display Inducible Gene Expression in Response to Beneficial Elements, Metal, and Metalloid Ions. *Front Plant Sci*. 7;8:129.

Evsyutina, D.V.; Fisunov, G.Y.; Pobeguts, O.V.; Kovalchuk, S.I.; & Govorun, V.M. (2022). Gene Silencing through CRISPR Interference in Mycoplasmas. *Microorganisms. 10*, 1159.

Fang, G., Bhardwaj, N., Robilotto, R., & Gerstein, M.B. (2010). Getting started in gene orthology and functional analysis. *PLoS Comput Biol.* 26;6(3):e1000703.

Fang G, Rocha E, Danchin A. (2005). How Essential Are Nonessential Genes?. *Molecular Biology and Evolution*, 2147–2156.

Farzam, K., Nessel, T.A, & Quick, J. (2022). Erythromycin. In: StatPearls [Internet]. Treasure Island.

Fen, L. (2021). Effects of NaCl Concentrations on Growth Patterns, Phenotypes Associated With Virulence, and Energy Metabolism in Escherichia coli BW25113

François, G. (2014). Biochemical Ecotoxicology: Principles and Methods.

Garg, R., Tripathi, D., Kant., S, Chandra, H., Bhatnagar, R. & Banerjee, N. (2014). The Conserved Hypothetical Protein *Rv0574c* Is Required for Cell Wall Integrity, Stress Tolerance, and Virulence of Mycobacterium tuberculosis. *ASM Journals/Infection and Immunity*. 02274-14

Getahun, M., Blumberg, H.M., Ameni, G., Beyene, D & Kempker, R.R. (2022). Minimum inhibitory concentrations of rifampin and isoniazid among multidrug and isoniazid resistant *Mycobacterium tuberculosis* in Ethiopia. *PLoS ONE* 17(9): e0274426.

Giusto, N.M., Pasquaré, S.J., Salvador, G.A. & Ilincheta de Boschero, M.G. (2010). Lipid second messengers and related enzymes in vertebrate rod outer segments. *J Lipid Res*. (4):685-700.

Glaziou, P., Sismanidis, C., Floyd, K. & Raviglione, M. (2014). Global epidemiology of tuberculosis. *Cold Spring Harb Perspect Med*. 5(2):017798.

Glickman, S.M., Jacobs Jr, W.R. (2001). Microbial Pathogenesis of Mycobacterium tuberculosis: *Dawn of a Discipline*. P477-485.

Gonzalo-Asensio, J., Marinova, D., Martin, C. & Aguilo, N. (2017). MTBVAC: Attenuating the Human Pathogen of Tuberculosis (TB) Toward a Promising Vaccine against the TB Epidemic. *Front Immunol*. 15;8:1803.

Gopalaswamy, R. & Subbian, S. (2022). An Update on Tuberculosis Vaccines. Methods *Mol Biol.* 2410:387-409.

Graham, D.B. & Tripp, J. (2022). Ofloxacin. In: StatPearls [Internet]. Treasure Island

Hall, L., Jude, K.P., Clark, S.L & Wengenack, N.L. (2011). Antimicrobial susceptibility testing of Mycobacterium tuberculosis complex for first and second line drugs by broth dilution in a microtiter plate format. *J Vis Exp*. 24;(52):3094.

Hatzios, S.K., Baer, C.E., Rustad, T.R., Siegrist, M.S., Pang, J.M., Ortega, C., Alber, T., Grundner, C., Sherman, D.R. & Bertozzi, C.R. (2013). Osmosensory signaling in

Mycobacterium tuberculosis mediated by a eukaryotic-like Ser/Thr protein kinase. *Proc Natl Acad Sci U S A*. 24;110(52):E5069-77.

Hibbing, M.E., Fuqua, C., Parsek, M.R. & Peterson, S.B. (2010). Bacterial competition: surviving and thriving in the microbial jungle. *Nat Rev Microbiol*. 8(1):15-25.

Ijaq, J., Malik, G., Kumar, A. *et al.* (2019). A model to predict the function of hypothetical proteins through a nine-point classification scoring schema. *BMC Bioinformatics* **20**, 14

Jackson, M. (2014). The mycobacterial cell envelope-lipids. *Cold Spring Harb Perspect Med*. 7;4(10):a021105.

Joshi, J.M. (2011). Tuberculosis chemotherapy in the 21 century: Back to the basics. *Lung India.* 28(3):193-200.

Kalscheuer, R., Palacios, A., Anso, I., Cifuente, J., Anguita, J., Jacobs, W.R Jr., Guerin M.E. & Prados-Rosales, R. The *Mycobacterium tuberculosis* capsule: a cell structure with key implications in pathogenesis. *Biochem J.* (14):1995-2016.

Kamal, F., Zhang, L., & Reha-Krantz, L.J. (2013). Escherichia coli XL10-gold bacteria produce bacteriophage. *J Clin Microbiol*. 51(2):727.

Klumpp, S. & Hwa, T. (2014). Bacterial growth: global effects on gene expression, growth feedback and proteome partition. *Curr Opin Biotechnol*. 96-102.

Kooijman, E.E. & Burger, K.N. (2009). Biophysics and function of phosphatidic acid: a molecular perspective. *Biochim Biophys Acta*. 1791(9):881-8.

Kootery, K.P., & Sarojini, S. (2022). Structural and functional characterization of a hypothetical protein in the RD7 region in clinical isolates of Mycobacterium tuberculosis — an in silico approach to candidate vaccines. *J Genet Eng Biotechnol* 20, 55.

Kowalska-Krochmal, B. & Dudek-Wicher, R. (2021). The Minimum Inhibitory Concentration of Antibiotics: Methods, Interpretation, Clinical Relevance. *Pathogens.* 10(2):165.

Larrouy-Maumus, G., Leonardo, B., Marino, Ashoka, V. R. Madduri, T. J., Ragan, Debbie M. Hunt, Lucrezia Bassano, Maximiliano G. Gutierrez, D. Branch Moody, Fernando R.

Pavan, & Luiz Pedro S. de Carvalho. (2016). Cell-Envelope Remodeling as a Determinant of Phenotypic Antibacterial Tolerance in *Mycobacterium tuberculosis ACS Infectious Diseases 2* (5), 352-360

Loerger, T.R., Feng, Y., Ganesula, K., Chen, X., Dobos, K.M., Fortune, S., Jacobs, W.R Jr., Mizrahi, V., Parish, T., Rubin E, Sassetti C, Sacchettini J.C. (2010). Variation among genome sequences of H37Rv strains of Mycobacterium tuberculosis from multiple laboratories. *J Bacteriol*. (14):3645-53.

Luca, S., & Mihaescu, T. (2013). History of BCG Vaccine. *Maedica (Bucur).* 8(1):53-8.

Lynn, G., Dover, A.M., Cerdeño-Tárraga, M.J., Pallen, Julian Parkhill, Gurdyal, B. (2004). Comparative cell wall core biosynthesis in the mycolated pathogens, *Mycobacterium tuberculosis* and *Corynebacterium diphtheriae*, *FEMS Microbiology Reviews*, 225–250.

MacGilvary, N.J., Kevorkian,. YL, Tan, S. (2019). Potassium response and homeostasis in *Mycobacterium tuberculosis* modulates environmental adaptation and is important for host colonization. *PLoS Pathog* 15(2): e1007591.

Maitra, A., Munshi, T., Healy, J., Martin, L.T, Vollmer W, Keep NH, Bhakta S. (2019). Cell wall peptidoglycan in *Mycobacterium tuberculosis*: An Achilles' heel for the TB-causing pathogen, *FEMS Microbiology Reviews*, 548–575.

Mazandu GK, Mulder NJ. Function prediction and analysis of mycobacterium tuberculosis hypothetical proteins. Int J Mol Sci. 2012;13(6):7283-302. doi: 10.3390/ijms13067283. Epub 2012 Jun 13. PMID: 22837694; PMCID: PMC3397526.

Mérida, I., Avila-Flores, A., Merino, E. (2008). Diacylglycerol kinases: at the hub of cell signalling. *Biochem J*. 1;409(1):1-18.

Mishra, A., & Surolia, A. Mycobacterium tuberculosis: Surviving and Indulging in an Unwelcoming Host. *IUBMB Life* (2018) 70:917–25.

Mishra, S. (2009). Function prediction of Rv0079, a hypothetical Mycobacterium tuberculosis DosR regulon protein. *J Biomol Struct Dyn*. 27(3):283-92.

Mistry, J., Chuguransky, S., Williams, L., Qureshi, M., Salazar, G.A, Sonnhamme,r E..LL, Tosatto, S.C.E, Paladin L, Raj S, Richardson LJ, Finn RD, Bateman A. (2021). Pfam: The protein families database in 2021. *Nucleic Acids Res*. 8;49(D1):D412-D419.

Möbius, K., Kazemi, S., Güntert, P., Jakob A, Heckel A, Becker-Baldus J, Glaubitz C. (2019). Global response of diacylglycerol kinase towards substrate binding observed by 2D and 3D MAS NMR. *Sci Rep*. 8;9(1):3995.

Mohan, R., Venugopal ,S. (2012). Computational structural and functional analysis of hypothetical proteins of Staphylococcus aureus. *Bioinformation*. 8(15):722-8.

Müller, H., Mancuso, F. (2008). Identification and analysis of co-occurrence networks with NetCutter. *PLoS One*. (9):e3178.

Myrbråten, I.S, Will, K., Salehian, Z., Håvarstein L.S, Straume D., Mathiesen, G, Kjos ,M. (2019). CRISPR Interference for Rapid Knockdown of Essential Cell Cycle Genes in Lactobacillus plantarum. *mSphere*. 20;4(2):e00007-19.

National Instistute of allergy and infectious diseases. 2016. Tuberculosis drugs and mechanism of action.

Naveed, M, Makhdoom, S.I, Abbas, G, Safdari, M, Farhadi A, Habtemariam S, Shabbir MA, Jabeen K, Asif MF, Tehreem S. The Virulent Hypothetical Proteins: (2022). The Potential Drug Target Involved in Bacterial Pathogenesis. *Mini Rev Med Chem*. (20):2608-2623.

Niederweis, M., Danilchanka, O., Huff, J., Hoffmann, C., Engelhardt H. (2010). Mycobacterial outer membranes: in search of proteins. *Trends Microbiol*. (3):109-16.

O'Connor C, Brady MF. (20220. Isoniazid. StatPearls [Internet]. Treasure Island (FL): StatPearls

Palomino, J.C., Martin, A. (2014). Drug Resistance Mechanisms in Mycobacterium tuberculosis. Antibiotics (Basel). 2;3(3):317-40

Pang, Y., Lu, J., Wang, Y., Song, Y., Wang, S., Zhao, Y. (2013). Study of the rifampin monoresistance mechanism in Mycobacterium tuberculosis. *Antimicrob Agents Chemother*. 57(2):893-900.

Parbhoo, T., Mouton, J.M, Sampson, S.L. (2022). Phenotypic adaptation of Mycobacterium tuberculosis to host-associated stressors that induce persister formation. *Front Cell Infect Microbiol*. 27;12:956607.

Pavelka MS Jr, Mahapatra S, Crick DC. Genetics of Peptidoglycan Biosynthesis. Microbiol Spectr. 2014 Aug;2(4):MGM2-0034-2013. doi: 10.1128/microbiolspec.MGM2-0034-2013. PMID: 26104213.

Penewit, K., Salipante, S.J. (2020). Genome Editing in Staphylococcus aureus by Conditional Recombineering and CRISPR/Cas9-Mediated Counterselection. Methods *Mol Biol.* 2050:127-143.

Pérez, I., Uranga, S., Sayes, F., Frigui, W., Samper, S., Arbués A, Aguiló N, Brosch R, Martín C, Gonzalo-Asensio J. (2020). Live attenuated TB vaccines representing the three modern Mycobacterium tuberculosis lineages reveal that the Euro-American genetic background confers optimal vaccine potential. *EBioMedicine.* 55:102761.

Peters, J.M, Colavin, A., Shi, H, Czarny, T.L, Larson, M.H, Wong, S, Hawkins, J.S, Lu, C.H.S., Koo, B.M, Marta, E, Shiver, A.L, Whitehead, E.H, Weissman JS, Brown ED, Qi LS, Huang KC, Gross CA. (2016). A Comprehensive, CRISPR-based Functional Analysis of Essential Genes in Bacteria. *Cell.* (6):1493-1506.

Raj, U., Sharma, A.K., Aier, I. et al. (2017). In silico characterization of hypothetical proteins obtained from Mycobacterium tuberculosis H37Rv. Netw Model Anal Health Inform *Bioinforma* 6, 5.

Rebollo-Ramirez, S, & Larrouy-Maumus, G. NaCl triggers the CRP-dependent increase of cAMP in Mycobacterium tuberculosis.*Tuberculosis,* 8-16.

Rock, J.M., Hopkins, F.F., Chavez, A., Diallo, M, Chase, M.R, Gerrick, E.R, Pritchard, J.R, Church, G.M, Rubin, E.J, Sassetti, C.M, Schnappinger, D, Fortune, S.M. (2017). Programmable transcriptional repression in mycobacteria using an orthogonal CRISPR interference platform. *Nat Microbiol*. 6;2:16274.

Rodwell, T.C, Kapasi, A.J, Moore, M., Milian-Suazo, F, Harris, B., Guerrero, L.P, Moser, K, Strathdee, S.A, Garfein, R.S. (2009). Tracing the origins of *Mycobacterium bovis* tuberculosis in humans in the USA to cattle in Mexico using spoligotyping. *Int J Infect Dis*. 3:e129-35.

Rojas, E.J.I., Kryazhimskiy, S., NguyenBa, A.N. and Desai, M.M. (2019) Modular epistasis and the compensatory evolution of gene deletion mutants. *PLoS Genet* 15, e1007958.

Roy, A, Eisenhut, M, Harris, R.J, Rodrigues, L.C, Sridhar, S, Habermann, S, Snell, L, Mangtani, P, Adetifa I, Lalvani A, Abubakar I. (2014). Effect of BCG vaccination against Mycobacterium tuberculosis infection in children: systematic review and meta-analysis. *BMJ*. 5;349:g4643.

Sakane, F, Hoshino ,F, Murakami, C. (2020). New Era of Diacylglycerol Kinase, Phosphatidic Acid and Phosphatidic Acid-Binding Protein. *Int J Mol Sci*. 6794.

Salzberg, S.L. (2019). Next-generation genome annotation: we still struggle to get it right. *Genome Biol* **20**, 92.

San Diego State University. Biological and Medical Informatics Research Center (BMIRC)

Schwan, W.R, Lee, J.L, Lenard, F.A, Matthews, B.T, Beck, M.T. (2002). Osmolarity and pH growth conditions regulate fim gene transcription and type 1 pilus expression in uropathogenic Escherichia coli. *Infect Immun*. 1391-402.

Scriba, T.J, Netea, M.G, Ginsberg, AM. (2020). Key recent advances in TB vaccine development and understanding of protective immune responses against Mycobacterium tuberculosis. *Semin Immunol*. 50:101431..

Seung, K.J, Keshavjee, S, Rich M.L. (2015). Multidrug-Resistant Tuberculosis and Extensively Drug-Resistant Tuberculosis. *Cold Spring Harb Perspect Med*. 5(9):a017863.

Shandil, R.K., Jayaram, R., Kaur, P., Gaonkar, S, Suresh, B.L, Mahesh, B.N, Jayashree R, Nandi, V, Bharath, S, Balasubramanian, V. (2006). Moxifloxacin, ofloxacin, sparfloxacin, and ciprofloxacin against Mycobacterium tuberculosis: evaluation of in vitro and

pharmacodynamic indices that best predict in vivo efficacy. *Antimicrob Agents Chemother.* (2):576-82

Shirai, Y., & Saito, N. (2014). Diacylglycerol kinase as a possible therapeutic target for neuronal diseases. *J Biomed Sci* **21**, 28

Sia, I.G, & Wieland, M.L. (2011). Current concepts in the management of tuberculosis. *Mayo Clin Proc*. 86(4):348-61.

Singh, R, Dwivedi, S.P.D, Gaharwar, U.S., Meena R., Rajamani P., Prasad T. (2020). Recent updates on drug resistance in *Mycobacterium tuberculosis*. *J. Appl. Microbiol.*, 128 (2020), pp. 1547-1567

Sloan, D.J, Davies, G.R, Khoo, S.H. (2013). Recent advances in tuberculosis: New drugs and treatment regimens. *Curr Respir Med Rev*. 9(3):200-210.

Smith, I. (2003). *Mycobacterium tuberculosis* pathogenesis and molecular determinants of virulence. *Clin Microbiol Rev*. 463-96.

Sotgiu, G., Centis, R., D'ambrosio, L., Migliori, G.B. (2015). Tuberculosis treatment and drug regimens. *Cold Spring Harb Perspect Med*. 017822.

Stylianou, E., Griffiths, K.L., Poyntz, H.C., Harrington-Kandt, R., Dicks, M..D, Stockdale, L., Betts, G., McShane, H. (2015). Improvement of BCG protective efficacy with a novel chimpanzee adenovirus and a modified vaccinia Ankara virus both expressing Ag85A. *Vaccine*. 6800-8.

Sullivan, T., & Ben Amor, Y. (2016). Global Introduction of New Multidrug-Resistant Tuberculosis Drugs-Balancing Regulation with Urgent Patient Needs. *Emerg Infect Dis*. 22(3):e151228.

Swain, S.S., Sharma, D., Hussain, T, & Pati S. (2020). Molecular mechanisms of underlying genetic factors and associated mutations for drug resistance in *Mycobacterium tuberculosis*. *Emerg Microbes Infect.* 9(1):1651-1663.

Tameris, M. D., Hatherill, M., Landry, B. S., Scriba, T. J., Snowden, M. A., Lockhart, S., et al. (2013). Safety and efficacy of MVA85A, a new tuberculosis vaccine, in infants

previously vaccinated with BCG: a randomised, placebo-controlled phase 2b trial. *Lancet* 381, 1021–1028.

Thakur, C.J, Saini, S., Notra, A., Chauhan, B., Arya, S., Gupta, R., Thakur, J., Kumar, V. Deciphering the functional role of hypothetical proteins from *Chloroflexus aurantiacs* J-10-f1 using bioinformatics approach. Mol Biol Res Commun. 2020 Sep;9(3):129-139. doi: 10.22099/mbrc.2020.36894.1495. PMID: 33313333; PMCID: PMC7727763.

Thakur, R., Naik, A., Panda, A., Raghu, P. (2019). Regulation of Membrane Turnover by Phosphatidic Acid: Cellular Functions and Disease Implications. Front. Cell Dev. Biol.,Sec. Membrane Traffic.00083

Thomas, M. & Daniel. (2006). The history of tuberculosis. *Respiratory Medicine*. 1862-1870.

Timmins, G.S. & Deretic, V. (2006). Mechanisms of action of isoniazid. *Mol Microbiol.* 62(5):1220-7.

Tong, Y., Jørgensen, T.S., Whitford, C.M. *et al.* (2021). A versatile genetic engineering toolkit for *E. coli* based on CRISPR-prime editing. *Nat Commun* **12**, 5206.

Unissa, A.N., & Hanna, L.E. (2017). Molecular mechanisms of action, resistance, detection to the first-line anti tuberculosis drugs: Rifampicin and pyrazinamide in the post whole genome sequencing era. *Tuberculosis*, 96-107.

Van Horn, W.D. & Sanders, C.R. (2012). Prokaryotic diacylglycerol kinase and undecaprenol kinase. *Annu Rev Biophys*. 41:81-101.

Vidal, G., Vidal-Céspedes, C., Silva, M.M., Castillo-Passi, C., Guillermo Yáñez Feliú, Fernán Federici, Timothy J.R. (2022). Accurate characterization of dynamic microbial gene expression and growth rate profiles, *Synthetic Biology*.20.

Wallace, R.J Jr, Nash, D.R, Steele, L.C, Steingrube, V. (1989). Susceptibility testing of slowly growing mycobacteria by a microdilution MIC method with 7H9 broth. *J Clin Microbiol.* 24(6):976-81.

Wang, Y., Wang, Z., Chen Y, Hua X, Yu Y, Ji Q. (2019). A Highly Efficient CRISPR-Cas9-Based Genome Engineering Platform in Acinetobacter baumannii to Understand the H_2O_2-Sensing Mechanism of OxyR. *Cell Chem Biol*. 19;26(12):1732-1742.e5.

Wattenberg, B.W, Raben DM. (2007). Diacylglycerol kinases put the brakes on immune function. *Sci STKE*. 7;2007(3980

Whitfield, M.G., Soeters, H.M., Warren, R.M, York, T, Sampson, S.L, Streicher, E.M, van Helden, PD, van Rie A. (2015). A Global Perspective on Pyrazinamide Resistance: Systematic Review and Meta-Analysis. *PLoS One*. 10(7):e0133869.

Whitlow, E.; Mustafa, A.S.; Hanif, S.N.M. (2020). An Overview of the Development of New Vaccines for Tuberculosis. *Vaccines* 586.

World Health Organization. 2020. Global Tuberculosis Report 2020. Geneva.

Yang, Z., Zeng, X., & Tsui, S. (2019). Investigating function roles of hypothetical proteins encoded by the Mycobacterium tuberculosis H37Rv genome. *BMC Genomics*. 20. 10.1186/s12864-019-5746-6.

Yao, J., & Rock CO. (2013). Phosphatidic acid synthesis in bacteria. *Biochim Biophys Acta.* 1831(3):495-502.

Zhang, R., Xu, W., Shao, S., & Wang, Q. (2021). Gene Silencing Through CRISPR Interference in Bacteria: Current Advances and Future Prospects. *Front Microbiol*. 31;12:635227.

Zhang, Y., Shi, W., Zhang, W. & Mitchison, D. (2013). Mechanisms of Pyrazinamide Action and Resistance. *Microbiol Spectr*. 2(4):1-12.

Zhao, C., Shu, X., & Sun, B. (2017). Construction of a Gene Knockdown System Based on Catalytically Inactive ("Dead") Cas9 (dCas9) in Staphylococcus aureus. *Appl Environ Microbiol*. 83(12):e00291-17.

Turnitin Report:

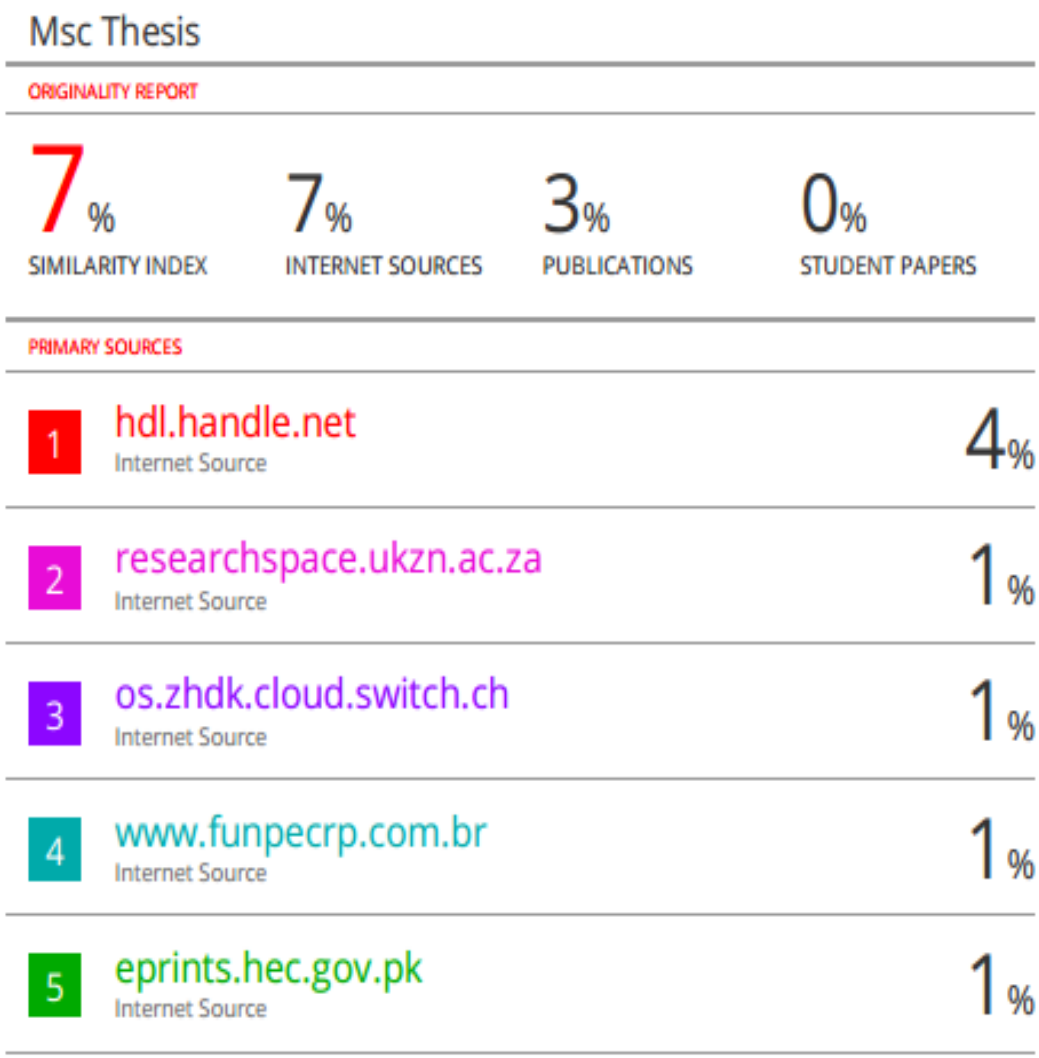

Msc Thesis

ORIGINALITY REPORT

7%	7%	3%	0%
SIMILARITY INDEX	INTERNET SOURCES	PUBLICATIONS	STUDENT PAPERS

PRIMARY SOURCES

1	hdl.handle.net Internet Source	4%
2	researchspace.ukzn.ac.za Internet Source	1%
3	os.zhdk.cloud.switch.ch Internet Source	1%
4	www.funpecrp.com.br Internet Source	1%
5	eprints.hec.gov.pk Internet Source	1%